Mechanisms of tree architecture construction: Analyses based on the pipe-model theory and biomechanics

（樹形の構築機構：パイプモデル理論と生体力学を基盤とした解析）

Kosei Sone

February, 2005

Department of Biology, Graduate School of Science,
Osaka University

Contents

Abbreviations

A	cross sectional area of the branch
A_B	cross sectional area of the branch at its base
A_f	cumulative leaf area of the branch
A_{FC}	mean cross sectional area of fiber cell
A_{FW}	cross sectional area occupied by fiber cell walls per unit xylem area
α	age of the branch
CT	control tree
CBs	control branches within the manipulated trees
d_{BB}	depth from the tree top to branch base
d_{LC}	depth from the tree top to the centre of leaf cluster
Δ_{AR}	average thickness between annual rings ($\Delta_{AR} = 0.5D_B/\alpha$)
ΔA	current-year growth of the branch cross sectional area
ΔN_f	yearly increment of leaf number on the branch
D	diameter of the branch
D_B	branch base diameter ($D_B = (D_{BH} + D_{BV}) / 2$)
D_{BH}	branch base diameter measured horizontally
D_{BV}	branch base diameter measured vertically
D_T	diameter of the main trunk at its base
E	elastic modulus
EI	flexural stiffness of the branch
F_B	bending force in the branch
F_C	compressive force parallel to the axis
F_m	gravitational force of the branch mass
g	acceleration of gravity
H	tree height
I	second moment of area of the branch
i	mean daily irradiance just above the branch
I_f	cumulative light interception of the branch ($I_f = A_f$ *RI)
i_f	cumulative light interception of the branch ($I_f = N_f * i$)
L_B	length of branch
L_{LA}	length of lever arm, from the base to the gravitational centre of the branch
L_s	length of current-year shoot
$\overline{Ls}$	average length of current-year shoots within the branch
L/T	number of long shoots relative to total number of current-year shoots
m	fresh mass of the branch
M	bending moment of the branch
MTs	manipulated trees
MBs	manipulated branches within the manipulated trees

N_f	leaf number on the branch
R	radius of curvature of the branch deflection
$1/R$	curvature of the branch deflection
R_{FW}	area of the cell walls relative to area of the fiber tissue
RI	irradiance just above the branch relative to that at open site
ρ	branch wood density (including barks)
θ	inclination of the branch axis from the vertical
σ	maximum stress in the branch
σ_C	compressive stress in the branch
σ_{max}	maximum bending stress in the branch
T_{FW}	mean thickness of cell walls of the fiber cells
VI	vigor index of the branch
W_f	cumulative leaf mass of the branch
Z	section modulus of the branch

General Introduction

Productive structure and self-thinning law of the plant stand

In dense plant stands, light and nutrient are resources that show more biased distributions than gaseous resources such as CO_2 and O_2. Light, the ultimate resource of photosynthesis, is attenuated steeply with depth from the surface of the plant stand due to interception and absorption by the leaves. Inversely, the leaves within the canopy tend to be arranged in a way that raises efficiency of photosynthetic production. Monsi and Saeki (1953, 2005) developed "the stratified-clipping method" to clarify the relationship between leaf arrangement and light attenuation. Briefly, the plant stand within a quadrate is vertically separated into several layers of a given thickness and the light intensities at the top of the respective layers are measured. The plants organs in the respective layers are cut separately and amounts of leaves and stems are measured. Vertical distributions of light intensity, leaves and of stems, obtained by this "stratified-clipping method," are plotted on the same diagram. Because this diagram clearly shows "structure" for photosynthetic production, this is called "the productive structure diagram" (Monsi and Saeki 1953, 2005).

The productive structure diagram greatly helps us to understand plant stands as the photosynthetic systems. For example, vertical foliage distributions differ between broad-leaved species and grasses. The broad-leaved species have less inclined or more horizontal leaves. Therefore, the foliage cluster is concentrated in the upper part of the stand. Thus, the light attenuation from the top to the bottom is very steep. Inversely, in grasses, foliage is more evenly distributed and light attenuation is more gradual. This relationship between the leaf inclination and light attenuation is very important for canopy photosynthesis. In strong light, canopy photosynthesis increases with the increase in leaf area index (LAI; cumulated leaf area per ground area, Hikosaka 2005, Hirose 2005), if leaves become more vertical with the increase in LAI. Leaf inclinations also differ within a plant stand. Leaves at upper positions of the stand tend to be vertical, while the leaves are more horizontal at lower positions, which contribute to homogenization of light absorption by the leaves. Moreover, leaves have ability to acclimate to their light environments and differentiate into sun and shade leaves

(Björkman 1981). In these ways, the photosynthetic system of the plant stand is optimized.

In the dense plant stand, light intensity steeply declines with canopy depth. Small individuals die in the shade due to shortage of light. Thus, if the stand is dense, density of individuals decreases with the stand growth, and the average size of the individual increases with time. This phenomenon is called self-thinning. Yoda et al. (1963) showed that the average biomass of a plant individual is proportional to 3/2 power of the individual density per ground area. This rule is called "3/2 power law of self-thinning".

The productive structure diagram clearly describes the photosynthetic system of the plant stand. On the other hand, the 3/2 self-thinning law revealed the rule of horizontal distribution of biomass in plant community. However, the structure of the plant community should be constructed based on both vertical and horizontal distributions of photosynthetic- and non-photosynthetic organs. Therefore, the direct relationship between leaves and stems should be clarified.

The pipe-model theory and *Leonardo da Vinci*'s rule

Although the productive structure diagram revealed significance of the distribution of photosynthetic organs, this diagram does not tell much about of the non-photosynthetic organs. Shinozaki et al. (1964*a*, *b*) found that, for a tree or even a forest canopy, the total leaf mass above a given plane is proportional to the sum of cross-sectional areas of stems cut by the plane (Shinozaki et al. 1964*a*, *b*). From this proportional relationship, Shinozaki et al. (1964*a*, *b*) proposed that a tree individual could be regarded as assemblage of "unit pipe system" which has unit amount of leaves and a stem pipe with corresponding thickness. This concept is called "the pipe-model theory" (Figure G-1).

On the other hand, *Leonardo da Vinci* found that the sum of cross-sectional areas of branches at any height equal to the cross-sectional area of the trunk (Richter 1970). This is called "*Leonardo da Vinci*'s rule" (Figure G-2).

In general, the above-mentioned proportional relationships are simply called the

pipe model. The pipe model has been used in many studies of tree growth modeling and of hydraulic architecture.

However, the thickness of the trunk generally increases towards the trunk base, in spite of the absence of leaves between the crown base and the trunk base. This phenomenon appears to violate the framework of the pipe-model theory. Shinozaki et al. (1964*a*, *b*) explained that this thickening reflects existence of the disused pipes. These pipes were connected to branches that have died back. The trunk tapering was also explanted from a mechanical viewpoint. Oohata and Shinozaki (1979) showed that the stem cross-sectional area was also proportional to its biomass including leaves and stems. This proportionality was valid not only for the branches within the crown but also for the trunk base. This proportional relationship indicates that if weight-force of the stem applied to the basal cross section vertically, the compressive stress is constant at any points within the tree. However, this assumption is not valid, because stems within a tree have diverse inclinations. Therefore, we have to consider bending moment to reveal the significance of mechanical tree design.

Mechanical models of tree design

Based on theories of mechanics, Greenhill (1881) calculated the critical buckling height of the tapering pole. Using the Greenhill's formula, McMahon (1973) computed the critical buckling height of the tree. Assuming that the ratio of elastic modulus to density of the material is constant, McMahon (1973) claimed that the critical buckling height of the tree is proportional to 2/3 power of the basal diameter of the trunk. Since these pioneering studies, many biomechanical studies have proposed mechanical models concerning tree architecture. These mechanical models have been used in many studies to argue significance of the tree architecture.

Most of these mechanical models assume that trees and branches within a tree have the same mechanical properties. This assumption is, however, invalid. Therefore, it is necessary to examine the actual mechanical status in various parts within a tree.

Branch autonomy

For clarifying mechanisms and ecological significance of the stem diameter growth, it is needed to analyze the photosynthetic production of each branch and translocation of the photosynthates within a tree. Photosynthates produced in leaves are translocated from these source leaves to other sink organs along a gradient in sugar concentration. However, photosynthates produced in a given branch are hardly translocated to its sibling branches, even when there is the gradient in sugar concentration between branches. This feature is called "branch autonomy" (Sprugel et al. 1991). The idea of branch autonomy has been used in many studies of the mechanisms of construction of tree architecture (Takenaka 1994, Perttunen et al. 1996, Day and Gould 1997) or of community structure (Takenaka 1994, King et al. 1997). However, it is misleading to treat all branches and shoots as being perfectly equal and perfectly autonomous. Growth of a shoot depends on its local light environment and its status among the neighboring daughter shoots within a branch (Goulet et al. 2000, Takenaka 2000, Sprugel 2002, Suzuki 2002, 2003, Nikinmaa et al. 2003).

The construction and maintenance of the branches, trunk, and root system rely on the photosynthates produced by young shoots. Photosynthesis and transpiration are the most important functions in studying tree growth and depend on irradiance. To understand how an entire tree is constructed, it is thus important to clarify light interception of each branch and the allocation pattern of photosynthates.

Aims of the present studies

The construction and maintenance mechanisms of the tree architecture based on the pipe-model theory and the mechanical and biological significance of such mechanisms have not been challenged. Understanding of these features should be very important for clarifying mechanisms of construction and maintenance of the plant community structure as well.

Thus, I conducted a series of studies. In Chapter 1, analyses of the branch diameter growth based on the pipe-model relationship are described. I used *Acer* trees, because they are deciduous and the diameter thickning of the species occur after the leaf development. Thus, the branch diameter growth would be largely attributed to

photosynthates produced in the same year. I have clarified that both photosynthetic production and branch status within a tree are important determinants of the branch thickening growth. In the study described in Chapter 2, I have examined the robustness of the pipe-model relationship employing the manipulations of branches that changed light intensity, leaf number, leaf area or shoot elongation in the field. I found that the pipe-model relationships were perturbed by the manipulations but, the next year of the manipulations, the pipe-model relationships were recovered. I also found that effects of the manipulations were also evident in the branches in which the manipulations were not applied. In such moderation of the effects of the manipulation and the recovery, relationships between the source and sink branches, and between the branches themselves and lower organs such as the trunk and roots, were greatly important. In the study described in Chapter 3, I examined biomechanical properties of branches and found marked differences in mechanical properties depending on the vertical positions and branch vigor within the tree, resulting in an adaptive tree design.

Based on these studies, construction and maintenance mechanisms of tree architecture based on the pipe-model theory and its mechanical and biological significance are discussed.

Pipe Model

Shinozaki et al. (1964)

stem cross-sectional area ∝ leaf amount

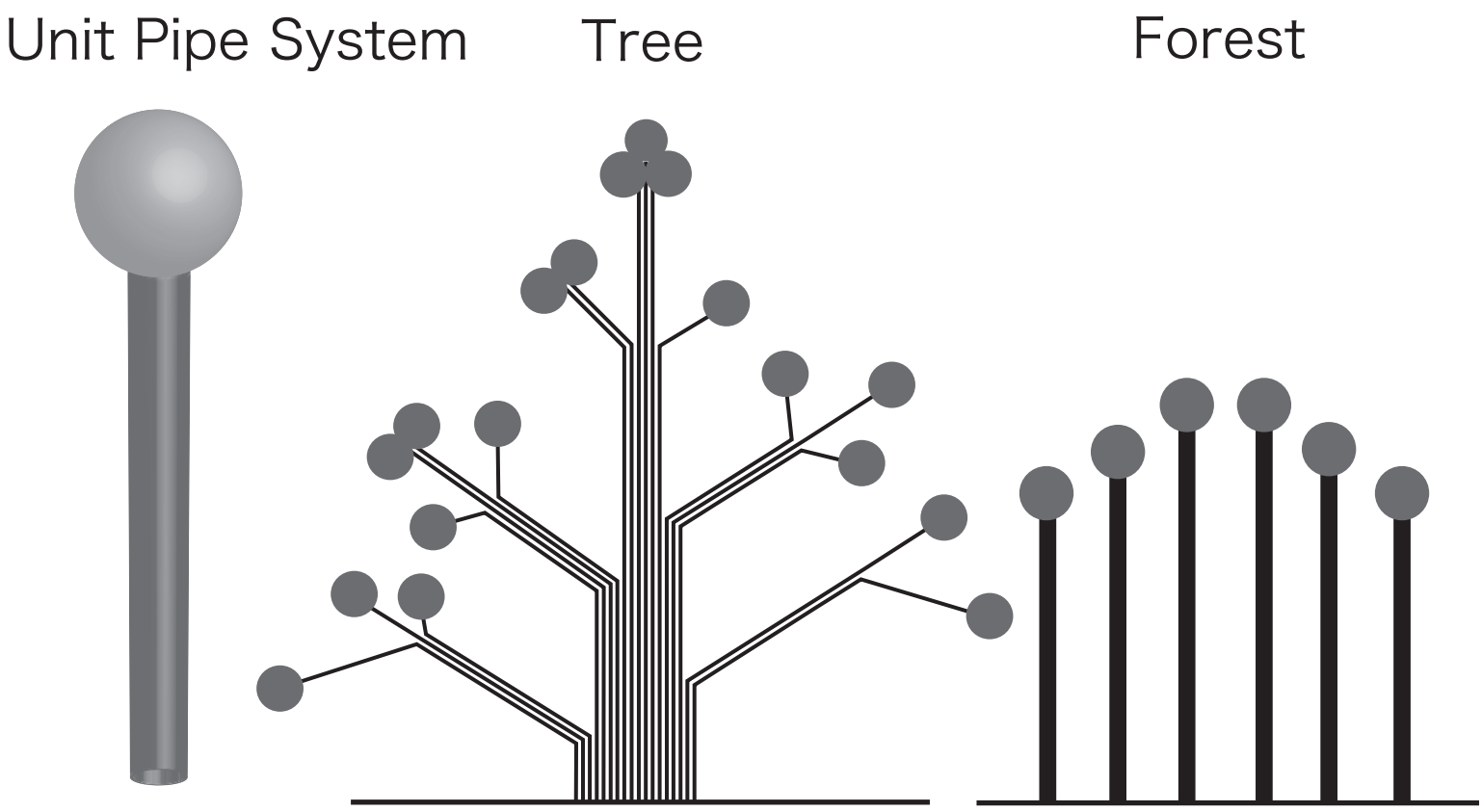

Figure G-1. Diagrams of the pipe-model theory. Left; unit pipe system. The sphere and cylinder represents a unit amount of leaves and a pipe of unit thickness. Middle; the pipe-model of tree architecture. A tree can be regarded as assemblage of the unit pipe systems. Right; the pipe-model for a forest community. The forest community can be also regarded as assemblage of the pipe-model of tree architecture (Shinozaki et al. 1964a, b).

Figure G-2. Sketches for branching rules by Leonardo da Vinci.

He mentioned that 'the sum of cross-sectional areas of branches at any height equals to the cross-sectional area of the trunk' (Richter 1970). This also means that, in a branching point, the sum of branch cross-sectional areas of daughter branches at immediately above the branching point equals to the branch cross-sectional area of the mother branch at immediately below the branching point.

Sketches are from 'The notebooks of Leonardo da Vinci' (Richter 1970).

(Chapter 1)

Dependency of branch diameter growth in young *Acer* trees on light availability and shoot elongation

Introduction

The cross-sectional area (or sapwood area) of a branch is proportional to the leaf mass or leaf area of the branch. This relationship had been noted by Leonardo da Vinci as long as 500 years ago (Richter 1970). On the basis of this proportional relationship, Shinozaki et al. (1964*a*, *b*) proposed that a tree is an assemblage of pipes having the same amount of leaves. This is called the pipe-model theory.

The pipe-model theory has been used in many studies that modeled tree growth (Valentine 1985, Mäkelä 1986, 1997, 1999, 2002; Chiba et al. 1988; Chiba 1990, 1991, Nikinmaa 1992, Chiba and Shinozaki 1994, Perttunen et al. 1996, 1998, Kershaw and Maguire 2000, Koskela 2000) and water conduction (Waring et al. 1982, Ewers and Zimmerman 1984*a*, *b*, Yamamoto and Kobayashi 1993). Several improvements to the pipe model have been suggested from the viewpoints of biomechanics and water conduction (Oohata and Shinozaki 1979, Chiba 1998, West et al. 1999, Berthier et al. 2001).

The ratio of leaf area (or leaf mass) to the sapwood area of the stem is, however, not always constant. The ratio differs depending on site conditions as well as the particular environment of a tree (Mäkelä et al. 1995, Mencuccini and Grace 1995, Berninger and Nikinmaa 1997, Carey et al. 1998, Mäkelä and Vanninen 1998, Li et al. 2000). The ratio tends to decrease with the increase in tree height (McDowell et al. 2002). The ratio also tends to decrease when the sapwood area is measured at the lower stem position (Mäkelä et al. 1995). These suggest that hydraulic conductance declines with the increase in path length and/or sapwood senescence.

Photosynthates produced in leaves are translocated from these source leaves to other sink organs along a gradient in sugar concentration. However, photosynthates produced in a given branch are hardly translocated to its sibling branches, even when there is the gradient in sugar concentration between branches. This feature is called "branch autonomy" (Sprugel et al. 1991). The idea of branch autonomy has been used in many studies of the mechanisms of construction of tree architecture (Takenaka 1994, Perttunen et al. 1996, Day and Gould 1997) or of community structure (Takenaka 1994, King et al. 1997). For example, Takenaka (1994) succeeded in mimicking the growth of a stand of trees by assuming that each autonomous shoot produces its daughter shoots or dies depending on the magnitude of its light interception.

However, it is misleading to treat all branches and shoots as being perfectly equal and perfectly autonomous. Growth of a shoot depends on its local light environment and its status among the neighboring daughter shoots within a branch (Takenaka 2000, Sprugel 2002). Goulet et al. (2000) proposed the vigor index (VI) to express the relative status of a branch. VI is calculated as follows. Consider a mother branch furcating several daughter branches at a branching point. The VI of the thickest branch among these daughter branches equals the VI of the mother branch. The VI of any other daughter branch is expressed as a product of the VI of the mother branch and the ratio of the cross-sectional area of this daughter branch to that of the thickest daughter branch. VI, thus, represents the relative size of each daughter branch. The calculation starts with the basal trunk and is repeated at every branching point. The VI values for the branch segments of the main axis of the tree are set to 1. Accordingly, VI decreases as branching order increases. When branch sizes are similar, the branches in the upper part of the crown generally have greater VI than those in the lower part of the crown (Goulet et al. 2000, Nikinmaa et al. 2003). In young trees of sugar maple (*Acer saccharum* Marsh.) and yellow birch (*Betula alleghaniensis* Britt.) (Goulet et al. 2000) and in Scots pine (*Pinus sylvestris* L. (*P. silvestris* L.)) (Nikinmaa et al. 2003), the growth of shoots depended on both their light environment and VI.

The construction and maintenance of the branches, trunk, and root system rely on the photosynthates produced by young shoots. Diameter growth of the branches downstream of the distal shoots would not be solely determined by the local conditions such as light interception or amount of leaves at the branch. In photosynthetically active

shoots, the ratio of photosynthates exported downwards to those used within the shoot would also vary from shoot to shoot. For these reasons, the allocation pattern of photosynthates should be more heterogeneous than that predicted by the pipe-model theory. To understand how an entire tree is constructed, it is thus important to clarify the allocation pattern of photosynthates. Although Valentine (1985), Mäkelä (1986, 1999, 2002), and Perttunen et al. (1996, 1998) developed plausible tree growth models that incorporated rules for the allocation of photosynthates, the rules per se have not been clarified. One of the potential mechanisms might be the abundance of long or leader branches that would show high levels of auxin synthesis. Auxin synthesized in young leaves and at active apices is directionally transported from the apices in the basal direction, and activates shoot elongation and the cambial function (Mohr and Schopfer 1995). Therefore, branches having long shoots or leaders would also show vigorous diameter growth. Such heterogeneous nature can be incorporated into the pipe-model paradigm. In their pioneering study, Morataya et al. (1999) found that leaf mass was correlated with area and volume growth of the sapwood in *Tectona grandis* L.f. and *Gmelina arborea* Roxb..

Photosynthesis and transpiration are the most important functions in studying tree growth and depend on irradiance. *In-situ* measurement of their rates for each shoot of the tree is not practical, but light interception can be accurately estimated for each shoot. An instantaneous photosynthetic light-response curve (the rate of photosynthesis plotted against irradiance) shows obvious light saturation. Daily photosynthesis plotted against daily photon flux density gives a much linearer curve (Terashima and Takenaka 1986). Moreover, leaves in a canopy can acclimate to their respective light environments (Björkman 1981). Therefore, the light interception by a shoot would be a reasonable index of the photosynthesis by a shoot for a long time period such as weeks or months (Campbell and Norman 1998).

In the present study, I used two maple species, *Acer mono* Maxim. var. *marmoratum* (Nichols) Hara f. *dissectum* (Wesmael) Rehder and *Acer rufinerve* (Sieb. & Zucc.), whose leaves have been shown to readily acclimate to their light environments (Hanba et al. 2002). I measured light interception by each current-year shoot for the index of photosynthetic production and transpiration. Then, I examined the:

(1) relationships between current-year growth of cross-sectional area of a branch and various leaf attributes, including leaf mass, leaf area, and light interception,
(2) relationships between current-year growth of cross-sectional area of a branch and the current-year increase in the leaves,
(3) patterns of allocation of carbon from shoot tips to the base of the trunk, and
(4) dependency of diameter growth of a branch on light intensity and the attributes of shoot growth activity (average length of the current-year shoots and VI).

On the basis of the results, I discuss mechanisms of the diameter growth of the branches and trunks.

Materials and methods

Study sites and species

The study was conducted in two deciduous, broad-leaved forests. One was the Ogawa Forest Reserve (36°56′N, 140°35′E, 600 m above sea level). The annual mean temperature is 9.0°C and the mean annual precipitation is 1800 mm. The other was the Ashu Experimental Forest of Kyoto University (35°20′N, 135°45′E, 700 m above sea level). The annual mean temperature is 12.3°C and the mean annual precipitation is 2400 mm.

Three *Acer mono* Maxim. var. *marmoratum* (Nichols) Hara f. *dissectum* (Wesmael) Rehder trees of 1–2 m (1.45 ± 0.37 m, mean ± S.D.) in height in the Ogawa Forest and six *A. rufinerve* (Sieb. & Zucc.) trees of 0.5–3 m (1.56 ± 0.86 m) in the Ashu Experimental Forest were selected from various light environments. The trees ranged from 3 to 15 years old and had not suffered from any injuries. The total number of current-year shoots examined was about 150 for *A. mono* and 350 for *A. rufinerve*. I used all these current-year shoots for analyses. Data were collected in 1997 for *A. mono* and in 1998 for *A. rufinerve*.

A. rufinerve is pioneer and *A. mono* is sub-climax species. Both are deciduous, broad-leaved, semi-shade-tolerant trees that often reach the forest canopy at maturity.

Their phyllotaxis is decussate and their branching pattern is monopodial (Sakai 1990). In both species, leaf expansion as well as the secondary growth of stems started in early May. The secondary growth finished between mid-August and mid-September in *A. mono* and in early September in *A. rufinerve* (Komiyama et al. 1987, 1989). Both species have diffuse-porous wood.

Measurement of the light environment

I assessed the light environments of all 500 current-year shoots in the field before leaf shedding. The relative irradiance of a given current-year shoot (RI_S), which is the ratio of irradiance measured just above the shoot to that measured at an open site, was obtained under diffuse light conditions, and RI_S was used as an index of the light environment of the shoot.

For *A. mono*, RI_S was estimated from hemispherical photographs (Pearcy 1989) analyzed using the software, HEMIPHOT (ter Steege 1994). I took hemispherical photographs just above each current-year shoot with a film camera (Nikomat, Nikon, Tokyo, Japan) fitted with a fish-eye lens (Fisheye, Nikon) on cloudy days in October 1997. The lens was kept horizontally when the photographs were taken. For current-year shoots that were too close to each other to allow us to take separate photographs, I took one photograph just above their center. From the hemispherical photographs, I calculated an indirect diffuse site factor (ISF) with HEMIPHOT. ISF was calculated on the assumption that the sky was uniformly overcast. I used ISF above each current-year shoot (ISF_S) as an index of RI_S. The highest value of RI_S in each of the three *A. mono* trees was 0.052, 0.142, and 0.189, respectively.

For *A. rufinerve*, I measured photosynthetically active photon flux density (PPFD; μmol photons m^{-2} s^{-1}) with quantum sensors (LI-190SB, LI-COR, Lincoln, NE, USA) in addition to the analysis with hemispherical photographs. These measurements were carried out on cloudy days in September 1998. I used two sensors. One was connected to a datalogger (Thermodac-E, Eto Denki Co., Ltd, Tokyo, Japan) and placed horizontally at a relatively open site on a forest road. The data were recorded every 5 s. The second sensor was kept horizontally just above the current-year shoot, and PPFD incident on the shoot ($PPFD_S$) was measured. The measurements with the two sensors

were carried out at the same time, and the ratio of PPFD above the shoot to that at the open site ($RPPFD_S$) was calculated (Messier and Puttonen 1995, Parent and Messier 1996). I also took a hemispherical photograph at the same open site where the first quantum sensor was placed, and calculated the ISF of the open site (ISF_O) with HEMIPHOT. I used ISF_O to correct RI_S (= ISF_S = $RPPFD_S$ × ISF_O) for each current-year shoot. The highest value of RI_S in each of the six *A. rufinerve* trees was 0.855, 0.722, 0.570, 0.299, 0.056, and 0.045, respectively.

For RPPFD < 0.7, instantaneous RPPFD under an overcast sky is strongly correlated with the mean daily RPPFD under a clear sky (r^2 = 0.872) as well as with the mean daily RPPFD under a overcast sky (r^2 = 0.969) (Messier and Puttonen 1995, Parent and Messier 1996). Thus, I did not take into account the effects of direct light.

Measurement of leaf attributes

I collected all leaves and measured the total leaf area on each current-year shoot (Af_S). For *A. mono*, I measured the leaf area with a leaf area meter (AAM-7, Hayashi Denko Co., Ltd, Tokyo, Japan). For *A. rufinerve*, I photocopied the leaves from each current-year shoot, digitized the images with a scanner (JX-250, Sharp, Osaka, Japan), and measured their areas with the NIH-Image v. 1.55 software (US National Institutes of Health). The product of Af_S and RI_S was regarded as the light interception by the current-year shoot ($If_S = Af_S \times RI_S$). The leaves were then dried at 80°C for 2 to 3 days and weighed to obtain the total leaf mass of the current-year shoot (Wf_S). These leaf attributes (Wf_S, Af_S, and If_S) are collectively referred to as F_S.

I estimated three leaf attributes for each branch: *Wf*, *Af*, and *If* (*F*). Each of the trees was notionally separated at every branching point and regarded as a fractal-like structure consisting of branch modules. A large branch module included many small branch modules, and the largest branch module in a tree was the tree itself. The weighted relative irradiance of a branch (RI) was calculated as *If*/*Af*.

I also counted the number of the current-year leaves in the branch (*Nf*) and the number of the leaf scars on the one-year-old branch in the whole branch. The latter equals to the previous-year leaf number in the branch (Nf_{-1}). I then estimated the current-year increment of the leaf number ($\Delta Nf = Nf - Nf_{-1}$). *Nf*, ΔNf, *F* and RI were

estimated for all branch modules in all trees.

Measurement of stem attributes

After collecting the leaves, I cut down the trees and brought them back to the laboratory. The lengths of all current-year shoots and of the branch segments between neighboring branching points were measured with a measuring tape. For very short samples, I used digital calipers (500-301, Mitutoyo Corporation, Kawasaki, Japan).

The greatest diameter (D) perpendicular to the length was measured at the base of each current-year shoot and at the middle point of each branch segment using the digital calipers. The diameters of the trunks at the bases of the crown and of the trunk were also measured. Using these diameters, I calculated the cross-sectional areas of the current-year shoots (A_S) and of the branch segments and trunk (A): A or $A_S = \pi D^2/4$. For A of the branch, A of the most basal branch segment within the branch or of the trunk just below the crown was used. Areas were estimated for all the branches of all the sample trees. All the branch and trunk cross-sections were wet and had a similar whitish color. Hence, there was no heartwood in the samples.

The current-year growth in cross-sectional area was estimated for each of the branches. To do so, I cut the branch segments or trunks at the position where the diameter was measured. At the greatest diameter of the section, I measured the diameter of the annual ring of the current year, excluding the bark and phloem, and that of the annual ring of the previous year. The annual rings were identified by using a loupe. The difference between the areas enclosed by the current-year and the previous-year annual rings was regarded as the current-year's growth in cross-sectional area of the branch segment or trunk (ΔA). For each branch, ΔA of the most basal branch segment within the branch or ΔA of the trunk just below the crown base was used. In some branch segments with very dense annual rings, the current-year thickenings were not estimated.

Status of each branch

The length of each current-year shoot was measured, and the mean length of the current-year shoot ($\overline{L_S}$) was obtained for each branch. The vigor index (VI) was

calculated according to Goulet et al. (2000).

Statistics

For all statistical analyses, I used StatView J-4.5 software (Abacus Concepts, Inc., Berkeley, CA, USA). I used a linear regression analysis for the relationships between leaf attributes and stem attributes. I also used multiple regression and partial correlation to test the dependency of the diameter growth of a branch on the light intensity (RI), average length of current-year shoots ($\overline{L_S}$), and vigor index (VI) of the branch.

Results

Cross-sectional branch area and area growth vs. leaf attributes

I analyzed the relationships between cross-sectional area (*A*) and leaf attributes (*F*) for all branch modules within the crowns (Figure 1-1). As leaf mass (*Wf*) or leaf area (*Af*) increased, *A* increased proportionally in both species (r^2 = 0.90–0.95). The coefficients of determination in the relationships between light interception (*If*) and *A* (r^2 = 0.78 and 0.87) were smaller than those for *Wf* and *Af*. The slopes of the relationships between *A* and *If* varied depending on the relative irradiances experienced by the trees. Trees growing in environments with high relative irradiance had smaller slopes for these relationships than those in low relative irradiance (The regression lines for respective irradiances are not shown).

When the current-year area growth of a branch (ΔA) was plotted against *F*, the data points were more scattered than those in Figure 1 (r^2 = 0.45–0.87) (Figure 1-2). It is, however, noteworthy that, in contrast to the results of the relationships between *A* and *F* (Figure 1-1), the coefficients of determination were clearly greater for *If* (r^2 = 0.75 and 0.87) than those for *Wf* (r^2 = 0.66 and 0.70) and *Af* (r^2 = 0.45 and 0.67).

Cross-sectional area growth of branch vs. leaf increment

If A is always proportional to F and there is no heartwood formation, current-year growth of cross-sectional area of the branch should be proportional to the annual increments in the leaf attributes (Valentine 1985, Mäkelä 1986). In Scots pine, Nikinmaa (1992) observed that difference in cross-sectional area growth of the trunks between just basipetal and acropetal of a given whorl was correlated with growth of the needle mass for the whorl. This observation implies that the amount of newly formed wood is correlated with the amount of new leaves.

We examined the relationships between the current-year cross-sectional area growth of a branch (ΔA) and the annual increment of the leaf number (ΔNf) (Figure 1-3). In *A. rufinerve*, proportionality in the relationships between ΔA and ΔNf (r^2 = 0.86) was stronger than that between ΔA and the current-year leaf number (Nf) (r^2 = 0.54). In *A. mono*, the proportionality was slightly stronger in the relationships between ΔA and ΔNf (r^2 = 0.67) than that between ΔA and Nf (r^2 = 0.61).

Patterns of carbon allocation from branch tip to trunk base

The pipe model assumes that the cross-sectional area of a branch is equal to the cumulative cross-sectional area of its daughter branches (Shinozaki et al. 1964*a*, Richter 1970, Nikinmaa 1992, Yamamoto and Kobayashi 1993). Thus, I analyzed the relationships between A and $\sum A$ and between ΔA and $\sum \Delta A$ for every branching point. For each branching point, A or ΔA of a branch segment at just basipetal to the branching point and $\sum A$ or $\sum \Delta A$ of all the branch segments at just acropetal to the branching point were measured and plotted (Figure 1-4). For the branching points within the crowns, A was almost identical to $\sum A$ of the daughter branches in both species (slope = 0.96 and 1.0, r^2 = 0.96 and 0.97). However, A values obtained at the trunk base tended to be larger than $\sum A$. In contrast, ΔA for the branching points within the crowns was smaller than $\sum \Delta A$ for the daughter branches in most cases (slope = 0.78 and 0.61), although the coefficient of determination for *A. mono* was not very large (r^2 = 0.93 in *A. rufinerve* and 0.60 in *A. mono*). However, again, ΔA values for basal trunks were larger than $\sum \Delta A$ for the daughter branches.

Dependency of branch diameter growth on light intensity and shoot growth activity

I analyzed the dependency of the branch diameter growth on its light environment and on the relative status of the branch. Relative irradiance (RI) was used as an index of the light environment of the branch. To indicate the relative status of a branch, we used the average length of its current-year shoots ($\overline{L_S}$) in the branch and the vigor index (VI) of the branch. With partial correlation and multiple regression analyses, we tested the effects of these parameters on the branch growth in cross-sectional area per unit of leaf area ($\Delta A/Af$).

$\Delta A/Af$ was correlated with $\overline{L_S}$ in both species (Table 1-1). Although $\Delta A/Af$ was correlated with RI in *A. rufinerve*, it was not significant in *A. mono*. VI had not effect on $\Delta A/Af$ in both species. There were not significant or not strong partial correlations among $\overline{L_S}$, RI, and VI (Table 1-1).

The multiple regression model used here is:

$$\Delta A/Af = b_0 + b_1(\mathrm{RI}) + b_2(\overline{L_S}) + b_3(\mathrm{VI}),$$

where b_0 is a constant and b_1, b_2, and b_3 are partial regression coefficients. The coefficient of determination (R^2) for *A. rufinerve* was larger than that for *A. mono* (Table 1-2). $\overline{L_S}$ was a significant determinant for both species. RI was significant only for *A. rufinerve*. VI was not significant in either species.

Discussion

Two assumptions of the pipe model are that there is a proportional relationship between branch cross-sectional area (or sapwood area) and leaf mass (or area), and that the sum of branch area just acropetal to a branching point equals the branch area just basipatal to the branching point. The results of this study indicate that these assumptions are generally valid (Figure 1-1 and left panels of Figure 1-4). Although it was reported for Scots pine (Nikinmaa 1992) and *Cryptomeria japonica* (L.f.) D. Don (Yamamoto and Kobayashi 1993) that the cross-sectional area of the trunk at the crown base was smaller than the sum of branch cross-sectional area, these trees were large (diameter > 10 cm)

and the stems included heartwood.

In the presented investigation, these two assumptions were not valid for the current-year growth in cross-sectional area. For the branches within the crowns, $\Delta A/\sum\Delta A$ was markedly smaller than 1, and $\Delta A/F$ gradually decreased with increment of branch size (Figure 1-2 and the right panels of Figure 1-4). These trends indicate that the diameter growth per unit of leaf area decreased toward the base. In other words, the carbon allocation decreased toward the basal direction within the crown.

The proportion of the current-year cross-sectional area growth to the cross-sectional area ($\Delta A/A$) generally decreases with increasing branch size and age. This fact and the constant $A/\sum A$ and A/F ratios explain that the slopes in the right panels of Figure 1-4 are smaller than 1. However, for the basal parts of the trunks, A was larger than $\sum A$ (left panels of Figure 1-4). Shinozaki et al. (1964*a*) explained that swelling of the trunk base is due to the accumulation of disused pipes (i.e., of heartwood). These pipes, according to their explanation, had been connected to old branches that died back. However, ΔA was larger than $\sum\Delta A$ at the trunk base (right panels of Figure 1-4). This means that material allocation increased toward the trunk base and that this also contributes to swelling of the trunk base. Other researchers have suggested that when the stems develop heartwood and the leaf turnover rate is faster than the rate of heartwood formation, newly formed sapwood area per unit of new leaf area decreases (Kershaw and Maguire 2000, Vanninen and Mäkelä 2000, Valentine 2001, Mäkelä 2002). This potentially explains the decrease in $\Delta A/\sum\Delta A$ with crown depth. However, in the present samples, there was no heartwood. If the age of the sapwood is greater than the leaf age, the leaves are connected to the older xylem as well as to the current-year xylem. It is always the case in deciduous *Acer* species having sapwood of multiple ages. This would at least partly explain the trend in the present study, in which $\Delta A/\sum\Delta A$ was smaller than 1 within the crown. The swelling at the trunk base would also contribute to mechanical support (Oohata and Shinozaki 1979) and to the increment of sapwood area per leaves (Mäkelä et al. 1995). It is probable that the inner xylem at the trunk base may gradually die back and have very low water conductivity.

The coefficients of determination between A and If were smaller than those for Wf and Af (Figure 1-1). In the shaded parts, A/If was larger. It was reported that the sap flow rate was higher in the outer xylem than in the inner xylem (Kozlowski and

Pallardy 1997, Domec and Gartner 2003). Sapwood of older stems in shaded site may show steeper radial gradient of water conductivity than that in bright sites. In contrast, *If* was a better determinant of ΔA than *Wf* or *Af* (Figure 1-2), indicating that light interception is more important for branch diameter growth than is leaf area or leaf mass. The strong relatioships between ΔA and *If* imply that the xylem produced in the current year would be a major pathway for the sap flow in these maple species.

On the other hand, ΔA was strongly dependent on the leaf number increment (ΔNf) in *A. rufinerve* (Figure 1-3). However, in *A. mono*, this relationship was not stronger than that between ΔA and *Nf*, and the plot patterns were similar to each other. These indicate that ΔNf are proportional to *Nf*. This phenomenon would be found in two cases. (1) Sample trees are very young and small and ΔNf is a major portion of *Nf*. (2) Sample trees are very old or located in the shaded sites. All shoots show little elongation, and leaf increment is very small and constant. Then, sink strength is homogenous among the branches within a tree. The case of *A. mono* trees was probably (1). The strong relationship between ΔA and ΔNf is consistent with the theoretical predictions (Valentine 1985, Mäkelä 1986). The above findings raise two questions: Which factor is important for stem diameter growth, light interception or leaf increment? What are the physiological mechanisms?

The diameter growth of branch per leaf area ($\Delta A/Af$) depended on RI in *A. rufinerve*, but not in *A. mono* (Tables 1-1 and 1-2). The reason for the poor dependency in *A. mono* could be due to the much smaller variation in RI observed in the *A. mono* in my study (RI = 0.007–0.189) than was observed in *A. rufinerve* (RI = 0.011–0.855). Hanba et al. (2002) showed that leaf mass per area (LMA) and photosynthetic capacity on a leaf-area basis increase with site irradiance in both of these *Acer* species. Thus, RI probably affected photosynthetic production in *A. mono* as well as in *A. rufinerve*.

It is noteworthy that $\Delta A/Af$ depended on the average length of the current-year shoots in the branch ($\overline{L_S}$) for both species (Tables 1-1 and 1-2). This means that the elongation rate of the whole branch was important for the diameter growth of the branch. Elongation of the current-year shoot would promote an annual increment in leaf number because long shoots generally have more leaves. Auxin, synthesized in active shoot apices and young leaves, is transported basipetally from the tips and activates branch elongation and cambial growth (Mohr and Schopfer 1995). It is highly probable that the

branch diameter growth was enhanced by auxin synthesized by many long shoots or leaders. On the other hand, many short shoots receiving strong light would be net producers (i.e. sources rather than sinks) of photosynthates and probably contributed to the growth of the trunk parts, in particular swelling of the trunk base and growth of the root system.

Goulet et al. (2000) and Nikinmaa et al. (2003) showed that shoot elongation depends on light intensity and on the vigor index (VI) of the shoot. In my results, the partial correlations among $\overline{L_S}$, RI and VI of the branch were not significant or not strong (Table 1-1). Moreover, VI of the branch was not a good determinant of ΔA of the branch. This was probably because the elongation and VI of respective shoots showed large variation even within a branch. Moreover, respective *L*s within branches with similar RI or VI differed considerably (data not shown). Some individual branches contained both long and short shoots, and both a leader and lateral daughter branches.

From these considerations, the major factor responsible for the leaf increment (ΔNf) would be shoot elongation ($\overline{L_S}$). Thus, the diameter growth of the branch (ΔA) within the crown would be determined by the balance between supply of photosynthates, which depends on light conditions (RI), and the demand created by the high cambial activity that was enhanced by vigorous shoot elongation ($\overline{L_S}$ or ΔNf).

Table 1-1. Partial correlation coefficients for the relationships between cross-sectional area growth per unit of leaf area ($\Delta A/Af$), relative irradiance (RI), average current-year shoot length ($\overline{L_S}$), and vigor index (VI) of branches of *A. rufinerve* and *A. mono.* $P < 0.05$ was considered significant. n.s. = not significant.

	Partial correlation coefficients			
	A. rufinerve (n = 193)		*A. mono* (n = 77)	
Relationship	*r*	*p*	*r*	*p*
$\Delta A/Af$ vs. RI	0.575	<0.0001	0.194	0.095 n.s.
$\Delta A/Af$ vs. $\overline{L_S}$	0.482	<0.0001	0.601	<0.0001
$\Delta A/Af$ vs. VI	0.031	0.670 n.s.	-0.137	0.241 n.s.
RI vs. $\overline{L_S}$	0.185	0.010	0.151	0.196 n.s.
RI vs. VI	0.050	0.492 n.s.	0.229	0.048
$\overline{L_S}$ vs. VI	0.123	0.090 n.s.	0.149	0.202 n.s.

Table 1-2. Partial and standardized regression coefficients for the multiple regression analysis of cross-sectional area growth per leaf area ($\Delta A/Af$) as a function of relative irradiance (RI), average shoot length ($\overline{L_S}$), and vigor index (VI) of branches of *A. rufinerve* and *A. mono*. $P < 0.05$ was considered significant. n.s. = not significant.

Explanatory variables	Partial regression coefficients	Standardized partial regression coefficients	P
A. rufinerve (n = 193, $R^2 = 0.710$, $P < 0.0001$)			
RI	1.766×10^{-4}	0.511	<0.0001
$\overline{L_S}$ (mm)	3.332×10^{-7}	0.404	<0.0001
VI	3.040×10^{-6}	0.017	0.673 n.s.
Intercept	1.236×10^{-5}	1.236×10^{-5}	0.017
A. mono (n = 77, $R^2 = 0.445$, $P < 0.0001$)			
RI	1.392×10^{-4}	0.162	0.095 n.s.
$\overline{L_S}$ (mm)	5.835×10^{-7}	0.605	<0.0001
VI	-7.668×10^{-6}	-0.107	0.241 n.s.
Intercept	2.420×10^{-5}	2.420×10^{-5}	0.0004

Note: The regression model is $\Delta A/Af = b_0 + b_1(\text{RI}) + b_2(\overline{L_S}) + b_3(\text{VI})$, where b_0 are constants, b_n are partial regression coefficients.

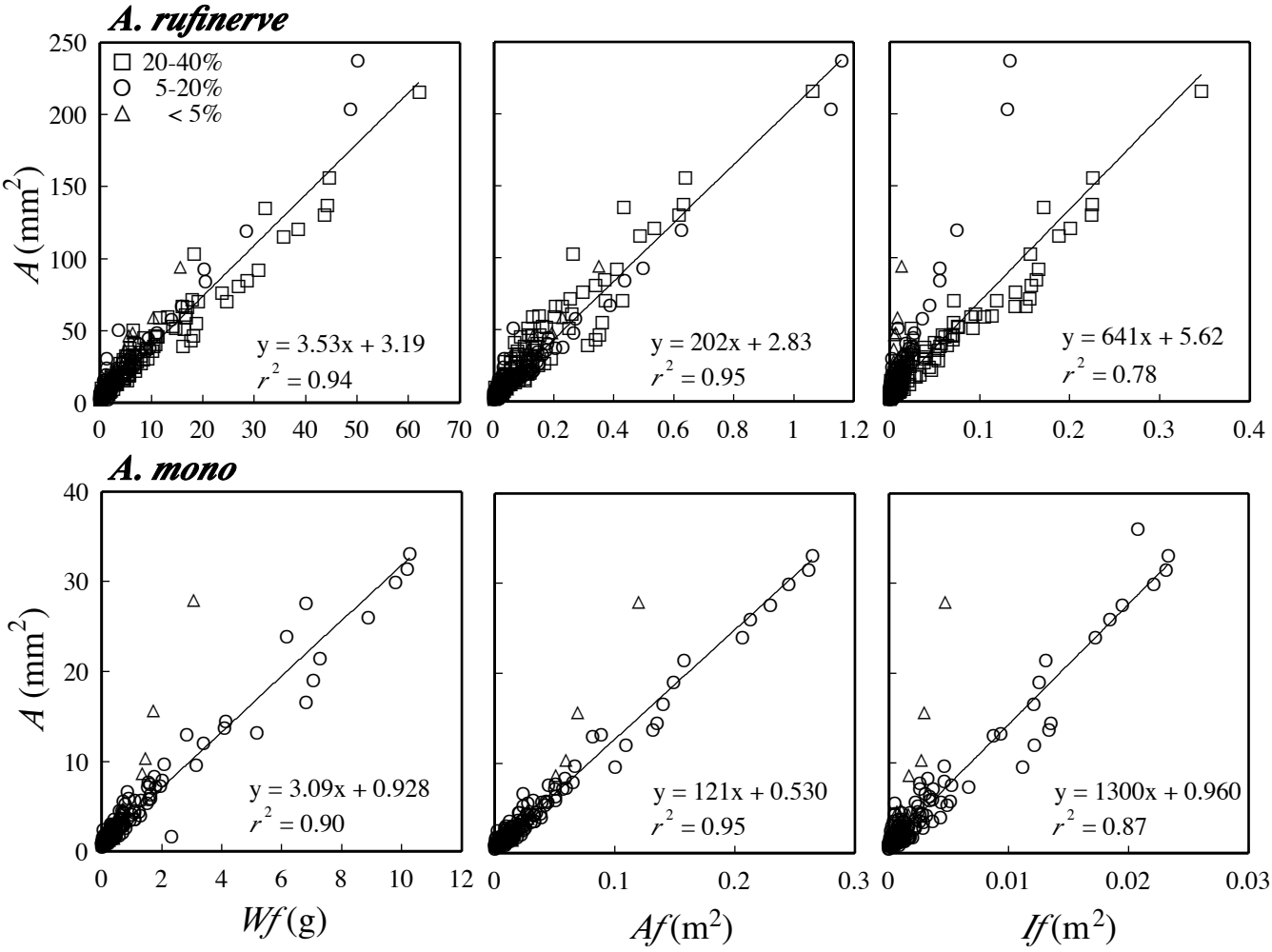

Figure 1-1. Relationships between branch cross-sectional area (*A*) and cumulative leaf parameters for a branch (*Wf*, *Af*, and *If*) within the crown. Data for six *A. rufinerve* trees and three *A. mono* trees are shown. Symbols denote the relative irradiance levels for the trees. Squares, circles, and triangles denote relative irradiance of 20%-40%, 5%-20%, and <5%, respectively. The regression lines were obtained without the data points for the trunk bases.

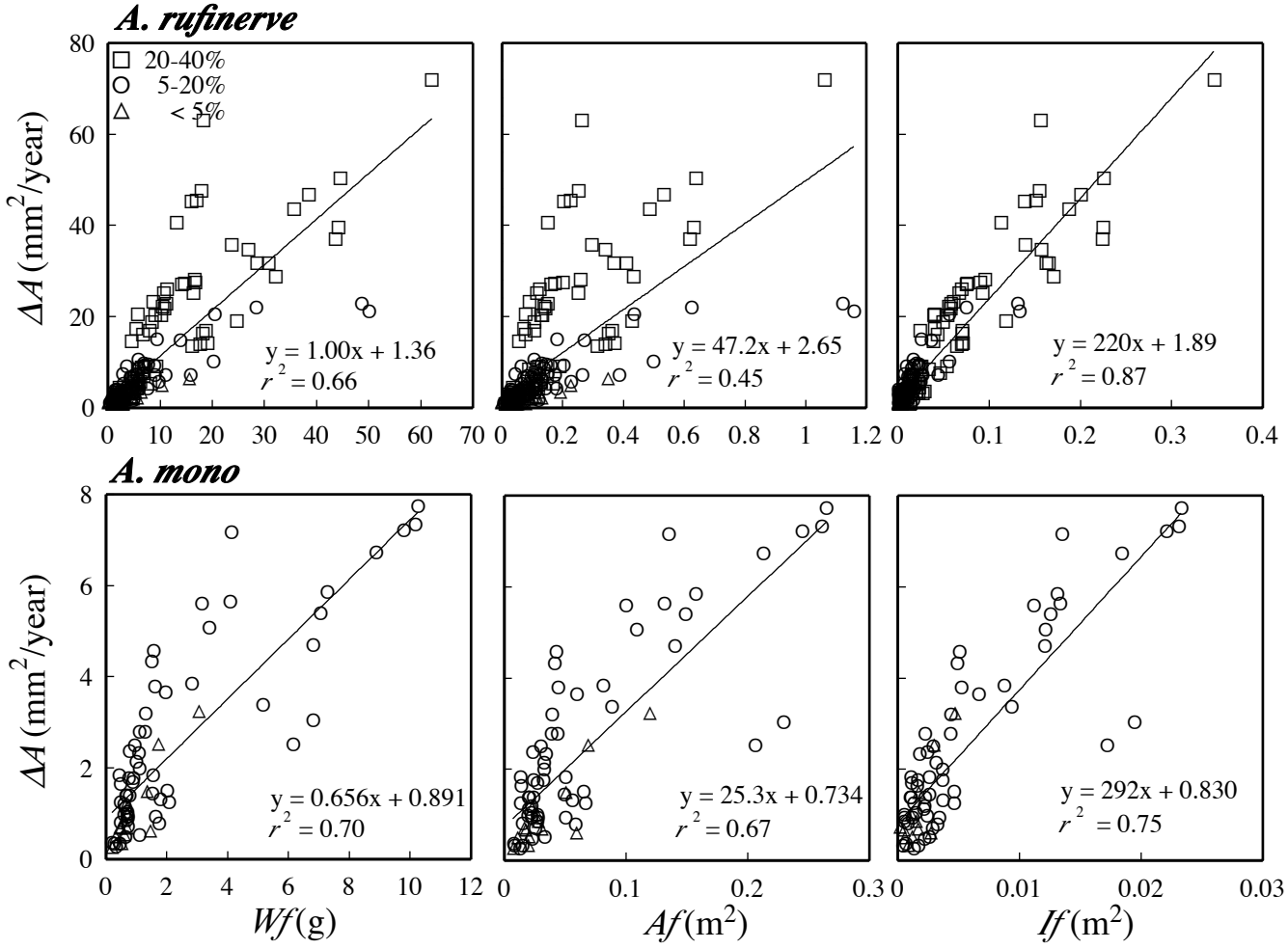

Figure 1-2. Relationships between current-year growth of branch cross-sectional area (ΔA) and cumulative leaf parameters for a branch (Wf, Af, and If) within the crown. For other information, see Figure 1-1.

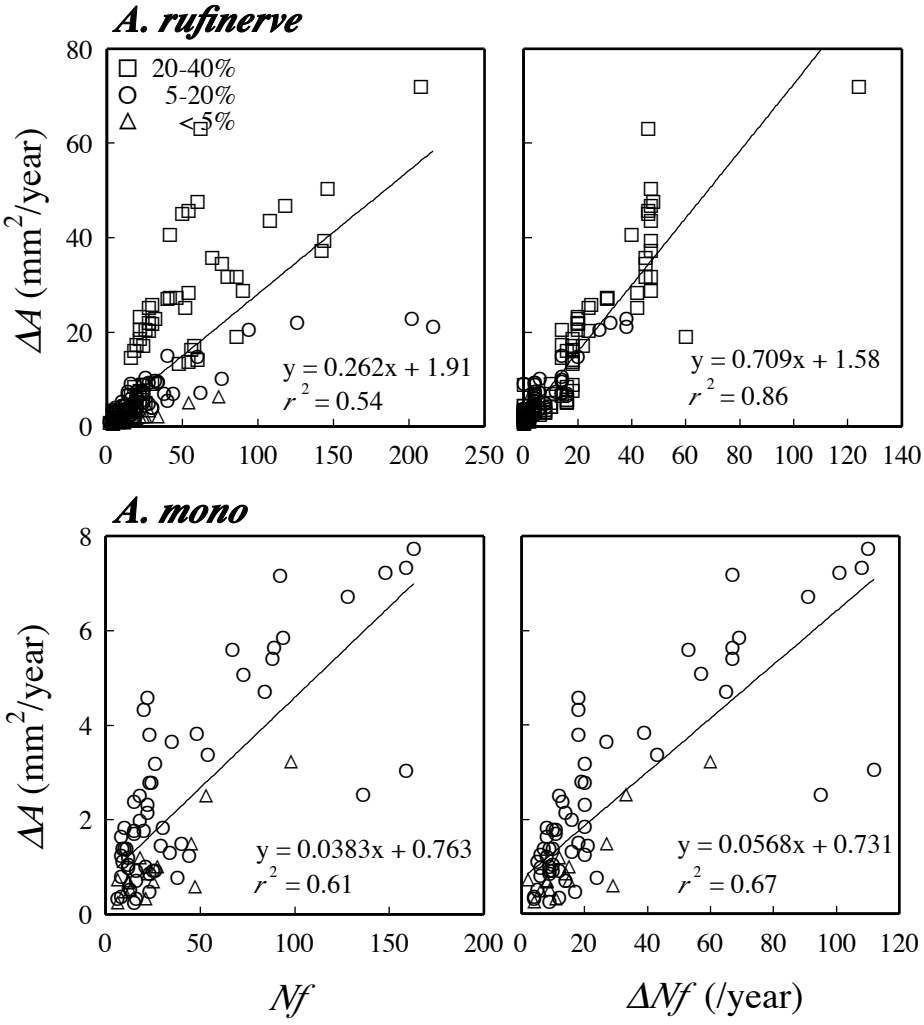

Figure 1-3. Relationships between current-year growth of branch cross-sectional area (ΔA) and current-year leaf number (Nf), and, between ΔA and annual increment in leaf number (ΔNf) within the crown. For other information, see Figure 1-1.

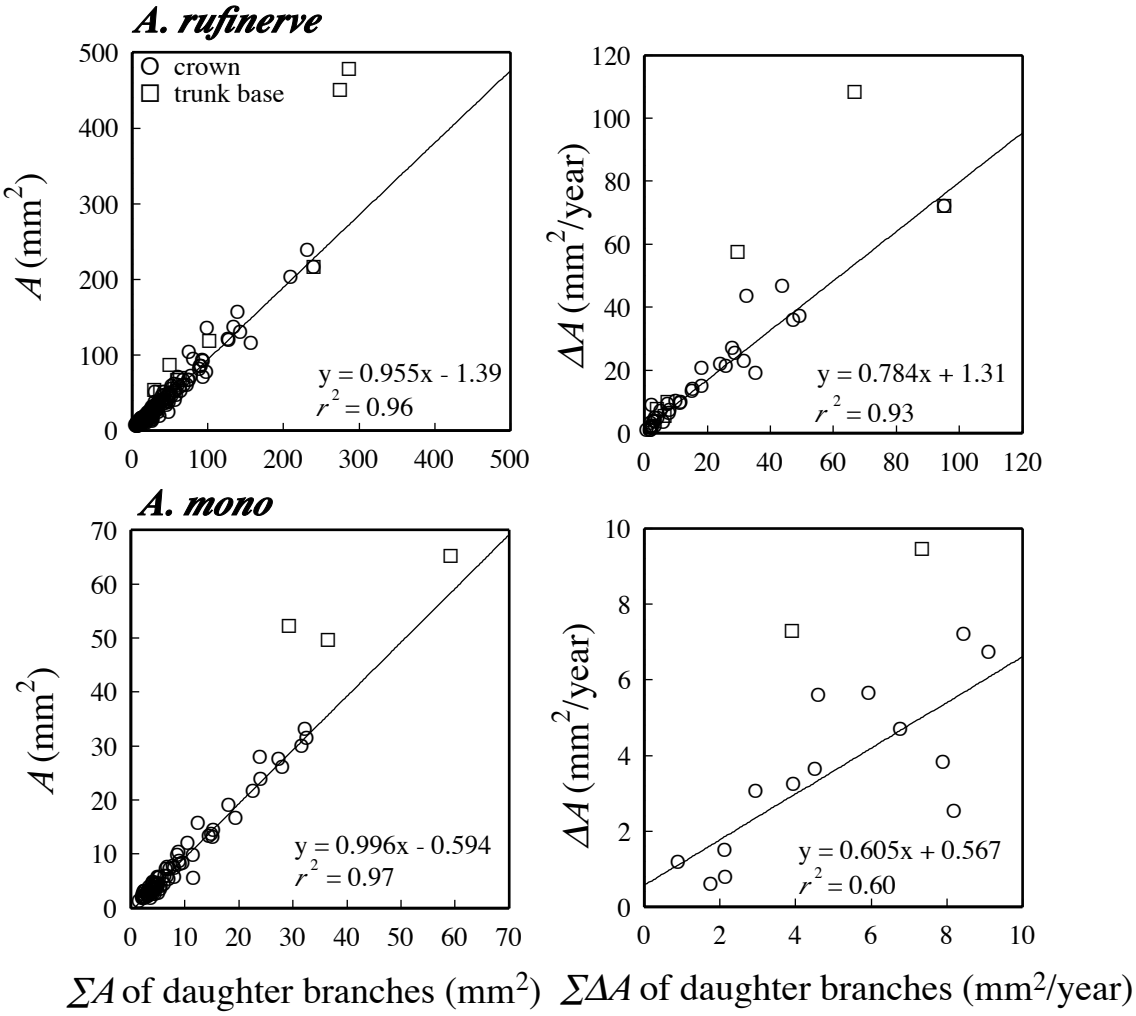

Figure 1-4. Relationships between branch cross-sectional area (A) and the sum of branch cross-sectional areas of daughter branches ($\sum A$) (left panels), and, between branch cross-sectional area growth (ΔA) and the sum of branch cross-sectional area growth of daughter branches ($\sum \Delta A$) (right panels). A and ΔA in the branch-segment just basipetal to each branching point and $\sum A$ and $\sum \Delta A$ of the daughter branch segments just acropetal to the branching point were measured and plotted. Data for six *A. rufinerve* trees and three *A. mono* trees are shown. The regression lines were obtained for the branches within the crowns excluding the trunk parts below the crowns (circles). Squares indicate the data for the basal trunk parts below the crowns.

(Chapter 2)

Responses of the pipe-model relationships in *Acer rufinerve* branches to artificial manipulations of light intensity, leaf amount and shoot elongation: Perturbation and recovery

Introduction

The pipe model theory of tree architecture indicates that a ratio of the total leaf area (or leaf mass) cumulated for the branch to the basal cross-sectional area (or sapwood area) of the branch is constant. The ratios of leaf area to sapwood area, however, differ depending on growth habitats (Mäkelä et al. 1995, Mencuccini and Grace 1995, Berninger and Nikinmaa 1997, Carey et al. 1998, Mäkelä and Vanninen 1998, Li et al. 2000). It was well documented that the ratios were lower in areas of arid climates (Mencuccini and Grace 1995, Berninger and Nikinmaa 1997). The ratios decreased with the increase in tree height (McDowell et al. 2002). The ratios were also low, when the sapwood area was measured at the trunk base rather than the crown base (Mäkelä et al. 1995). The latter two tendencies suggest that the hydraulic conductance declines with sapwood senescence and/or with the increase in the path length. In most of these studies, the variation in the ratio was discussed from a viewpoint of plant water relation, and roles of photosynthetic production and allocation of photosynthates in the pipe-model relationship have not been taken into account.

Although the pipe model relationships are usually obtained between the total leaf area (or leaf mass) cumulated for the branch and the basal cross-sectional area (or sapwood area) of the branch, in *A. rufinerve*, a strong relationship between the leaf number and the stem cross-sectional area of the branch was obtained (Figure 1-1 in Chapter 1, see also Figure 2-2). This is because variations in leaf area or in leaf dry mass among the leaves were not marked. The more important point is that this strong relationship is realized because the increase in leaf number on a branch obviously is

correlated with growth in the branch size as already shown in Chapter 1. Then, the mechanisms underlying the maintenance of the pipe-model architecture can be clarified by analyzing the relationships between the leaf number and the stem cross-sectional area.

It is widely observed that photosynthates produced by a given branch are transported preferentially to downstream organs including the trunk and roots and rarely transported to its neighbouring branches (Sprugel et al. 1991). However, this rule, called 'branch autonomy', does not suggest about an important point: how much photosynthates are transported to in the downstream organs. These shares appear to depend not only on its light environment but also on the status of the branch within the tree. As for shoot elongation, the importance of the relative status among branches was pointed out (Goulet et al. 2000, Takenaka 200, Sprugel 2002, Suzuki 2002, 2003, Nikinmaa et al. 2003). Actually, the analyses described in Chapter 1 clearly showed that the cross-sectional area growth of the branch depended on light interception and the increment in leaf number. The leaf number increment also strongly correlated with the branch growth rate such as elongation of the current-year shoots within the branch. Hence, branch growth depends on both supply of photosynthates and demand for photosynthates (Sone et al. 2005, Terashima et al. 2005, see also Terashima et al. 2002). The supply is further analyzed into the leaf amount and light intensity. The increment of the leaf amount and branch elongation should be important components of the demand for photosynthates within the branch. Then, it is important to know how these respective factors such as light intensity, leaf amount and shoot elongation interrelate to maintain the affect the pipe-model relationship. In the experiments in Chapter 2, I manipulated the light intensity, leaf amount and the shoot elongation of the branch and analyzed responses of the branch attributes.

Materials and Methods

Study site and plant materials

The study was conducted in a deciduous, broad-leaved forest (Ashu Experimental Forest, Kyoto University, 35˚20' stem N, 135˚45' E, 700 m a.s.l.), where the mean annual temperature is 12.3˚C and the mean annual precipitation is 2400 mm.

Five *A. rufinerve* (Sieb. et Zucc.) trees of 4 – 6 m in height were selected. In 2003, the total number of current-year shoots and branches examined were about 2800 and 170, respectively. We used all the current-year shoots for analyses. Data were collected in 2001, 2002 and in 2003.

A. rufinerve is a deciduous broad-leaved tree species that is pioneer and semi shade tolerant. Mature trees of this species often reach the forest canopies. The phyllotaxis is decussate and the branching pattern is monopodial (Sakai 1990). Leaf expansion and the secondary growth of stems start in early May. The secondary growth ceases in early September (Komiyama et al. 1987, 1989). This species has diffuse-porous wood. Sample trees used in this study did not develop the heartwood yet.

Measurement of light environment of branches

The light environments of 170 branches were assessed in the field from July to September in 2002 and 2003. Small pieces (15 * 25 mm) of the light sensitive film (Y-1 W, Pan, Taisei E&L, Tokyo) having the maximal sensitivity at 468 nm were attached on the leaves and collected after exposure for several weeks. Light transmittance of the film was measured before (T_0) and after (T) the exposure.

Mean daily irradiance i (MJ m^{-2} day^{-1}) was calculated as follws:

$$i = [-0.0101(100d/d_0)^2 - 0.5419(100d/d_0) + 167.59]/day,$$

Where, d_0 and d are:

$$d_0 = -1.4154 \log_{10}T_0 - 0.237$$

and

$$d = -1.4154 \log_{10}T - 0.237.$$

Measurement of leaf and stem attributes

Leaf and stem attributes were assessed in the field in November 2001, 2002 and 2003. In November, diameter growth of the branches and trunks ceased and green leaves were still on the branches in *A. rufinerve*. For each of the branches, the basal diameter (D) was measured with calipers. Numbers of leaf (N_f), current-year shoots and of

current-year long shoots were counted. Length of long shoots (*Ls*) was measured with a scale. The long shoots were defined as the shoots having four (two pairs) or more leaves. The branch cross-sectional area (A) was calculated as $A = \pi D^2/4$. The current-year growth of the branch cross-sectional area (ΔA) was calculated as the difference between the current-year A and previous-year A. The yearly increment of leaf number (ΔN_f) was similarly calculated as the difference between the current-year N_f and previous-year N_f. The light interception of the branch (i_f) was calculated as $i_f = N_f i$.

Design of branch manipulations

One tree was used as a control tree (CT) and the other four trees were subject to manipulations (manipulated trees, MTs). In each MT, the crown was divided into two branch clusters. Branches in one cluster were untreated (control branches, CBs), and those of the other cluster were subject to one of the manipulations (see below, manipulated branches, MBs). The branches including most vigorous axes (i.e., leader branches) were selected for MBs.

No manipulations were conducted in 2001. In May in 2002, MBs in MTs were subject to either of the manipulations (Figure 2-1):

***Shade*:** MBs within a MT were shaded by a frame (2.0 m width 2.5 m depth * 2.5 m height) covered with black shade cloths. Mean daily irradiance (i) in the shade box was about 15 % of the ambient i. By this manipulation, leaf numbers and leaf area in MBs did not change, but the light interception of the MBs decreased to 15 % of original levels.

***Half cut*:** For all the leaves on MBs in a MT, acropetal halves of the laminas were removed using scissors. By this manipulation, leaf numbers in MBs did not change, but the total leaf area of the MBs decreased to the half.

***Half pick*:** At each node in all the current-year shoots in MBs, one of the pair leaves was removed. By this manipulation, both leaf number and the total leaf area decreased to the half the original levels.

***Long-shoot pick*:** From each of the long shoots on MBs in a MT, leaves and stems were removed leaving the basal portions including the first two leaves (one pair). This manipulation artificially changed all the current-year shoots to short shoots. By this treatment, branch leaf number was reduced. Also, shoot elongation and the increase in

leaf area were suppressed.

In 2003, only the shade treatment was continued as was made in 2002 and the other manipulations were not conducted.

Results

Control tree

The cross-sectional area of the trunk at the crown base and total leaf number for the tree increased every year (Table 2-1). Very similar proportional relationships between the branch cross-sectional area (A) and leaf number of the branch (N_f) were observed every year (Figure 2-2 and 2-3). This indicates that the pipe-model relationship was maintained for these three years and that yearly growth in branch cross-sectional area (ΔA) was almost proportional to yearly increment of leaf number of the branch (ΔN_f) in the CT (Figure 2-6, see also Figure 1-3 in Chapter 1, Sone et al. 2005). Ratios of the branch cross-sectional area growth to leaf number ($\Delta A/N_f$) (Figure 2-4), light interception ($\Delta A/i_f$) (Figure 2-5) and to cumulative length of long shoot ($\Delta A/\sum Ls$) (Figure 2-7) did not differ between 2002 and 2003.

Shade manipulation

A increased every year in CBs and MBs (Table 2-1). In 2002, N_f also increased in both CBs and MBs, although the irradiance (i) for MBs decreased to 15%. In the second year of the shade treatment, 2003, N_f decreased in MBs. The increase in N_f was also suppressed in CBs, although CBs were not shaded.

The pipe-model relationship changed in response to the shade treatment (Figure 2-3). A/N_f was reduced by the shading in 2002. The ratio, however, recovered in 2003, although the shading continued in 2003 as well. The recovery was mainly attributed to the decrease in N_f (Table 2-1). Interestingly, a similar tendency was observed in CBs (Figure 2-3).

For either CBs or MBs, $\Delta A/N_f$ were similar between 2002 and 2003. $\Delta A/N_f$ were somewhat lower in MBs than in CBs. On the other hand, $\Delta A/i_f$ was smaller in 2003 than that in 2002 in both CBs and MBs. These indicate that MBs thickened despite of the considerable decrease in photosynthetic production in 2002. In 2003, N_f and shoot

elongation were suppressed and ΔA followed its photosynthetic production. Thus, $\Delta A/\Delta N_f$ did not differ between CBs and MBs in 2002 (Figure 2-6). The difference in $\Delta A/\sum Ls$ was not found in MBs between 2002 and 2003 (Figure 2-7). On the other hand, in CBs, the ratio in 2002 declined although CBs were not shaded. In MBs, the proportion of long shoots increased in 2002 and decreased in 2003. Inversely, in CBs, the proportion decreased in 2002 and increased in 2003 (Table 2-1).

Half cut manipulation

In CBs and MBs, A increased every year (Table 2-1). N_f increased in 2002 and decreased in 2003, although the leaves were not cut in 2003. The manipulation also affected characteristics of CBs.

A/N_f of the MBs significantly declined in 2002 (Figure 2-3) probably because leaf area and leaf mass decreased to half the original levels but the leaf number unchanged by this manipulation. The ratio recovered in 2003 mainly due to the decrement in leaf number (Table 2-1). Similar tendency was found in the CBs, although the leaves on CBs were not cut (Figure 2-3).

In both branches, $\Delta A/N_f$ and $\Delta A/i_f$ were smaller in 2002 than in 2003 (Figure 2-4 and 2-5). These decreases in 2002 were expected because the leaf area and leaf mass were reduced by the manipulation. Interestingly, these ratios also decreased in CBs. $\Delta A/\Delta N_f$ in CBs and MBs of the half cut MT in 2002 were smaller than that in the CT. Within the half cut MT, $\Delta A/\Delta N_f$ was significantly smaller in MBs than in CBs (Figure 2-6). This indicates that effects of the manipulation were stronger in MBs than in CBs. The long shoot proportion of the branch declined in both 2002 and 2003 in both CBs and MBs (Table 2-1). From MBs, the long shoots disappeared in 2003. In CBs, $\Delta A/\sum Ls$ in 2002 was considerably smaller than that in 2003 (Figure 2-7). This is because long shoot number decreased substantially in 2003.

Half pick manipulation

In both CBs and MBs, A increased every year (Table 2-1). In MBs, N_f increased in 2002, although the half of the leaves was removed. N_f markedly increased in 2003, because new axillary buds developed at axils of the removed leaves. In contrast, N_f of CBs decreased in 2003.

Although one half of the leaves were removed, the increase in A/N_f in 2002 was very small (Figure 2-3). The ratio recovered in 2003 by the increase in N_f (Table 2-1). In CBs, the increase in N_f was suppressed in 2002 and N_f decreased in 2003 (Table 2-1) and by the decrease in N_f, A/N_f slightly increased in 2003 (Figure 2-3).

In both branches, $\Delta A/N_f$ and $\Delta A/i_f$ in 2002 were similar to those in 2003 (Figure 2-4 and 2-5). These indicate that the decreased photosynthetic production limited the branch diameter growth. $\Delta A/\Delta N_f$ was greater in MBs than in CBs in 2002 (Figure 2-6). The reason was light intensity was greater in MBs than in CBs as is evident by comparison between Figure 2-4 and Figure 2-5. The long shoot proportion increased in 2002 and decreased in 2003 in both branches (Table 2-1). Because one MB showed little elongation but great thickening growth, the variance in $\Delta A/\sum Ls$ for MBs was very large in 2003 (Figure 2-7). When the data for this branch were excluded, there were only small changes between the years in both MBs and CBs, and $\Delta A/\sum Ls$ were smaller in MBs than in CBs in both years.

Long-shoot pick manipulation

In both CBs and MBs, A increased in both years (Table 2-1). In MBs, N_f increased in 2002, even though long shoots were removed. N_f markedly increased in 2003, because many long shoots developed in 2003. In contrast to the MBs, N_f decreased in 2003 and the long shoot proportion decreased in both years in CBs. The long-shoot pick manipulation of MBs in the previous year strongly affected development of long-shoots and the leaf amount of CBs (Table 2-1).

Interestingly, when both the leaf amount (area plus number) and the shoot elongation of the branch were suppressed by this manipulation, A/N_f did not change (Figure 2-3). The ratio increased in 2003 because the increase in N_f was smaller compared with stem growth (Table 2-1).

In both branches, $\Delta A/N_f$ and $\Delta A/i_f$ were almost similar between the two years (Figure 2-4 and 2-5). These indicate that photosynthetic production limited branch diameter growth. $\Delta A/\Delta N_f$ in MBs was slightly greater than that in CBs in 2002 (Figure 2-6). $\Delta A/\sum Ls$ in CBs was much larger in 2003 than in 2002. $\Delta A/\sum Ls$ in CBs in 2003 was greater than that in MBs in 2003 (Figure 2-7).

Discussion

The ratio expressing the pipe-model relationship (A/N_f) changed when the light intensity or the leaf amount of MBs was lowered without picking the long shoots (Figure 2-3). On the other hand, A/N_f did not change when both leaf amount and shoot elongation were suppressed by the *long-shoot pick* manipulation (Figure 2-3). Moreover, $\Delta A/\sum Ls$ did not vary much within MBs or CBs (Figure 2-7). These results indicate that the diameter growth strongly depended on shoot elongation within each branch. In Chapter 1, I have shown that the branch diameter growth depends on both supply of photosynthates relative to light interception, and demand for photosynthates which depends on the leaf number increment or shoot elongation (Sone et al. 2005, Terashima et al. 2005). The study described in this Chapter clearly showed importance of the long shoots as the factor closely relating to the demand for photosynthates.

Shoot elongation in MBs was little suppressed by the decrease in light intensity or that in the leaf amount (Table 2-1). In *A. rufinerve,* used in this study is a deciduous broad-leaved tree and the current-year shoots elongate mainly in May. Thus, materials for construction of the current-year shoots would mainly depend on stored photosynthates that were produced in the previous-year. For *Fagus japonica* Maxim., a deciduous broad-leaved tree, long shoot elongation depended not only on the previous-year light environment but also partly on the current-year light environment (Kimura et al. 1998, see also Terashima et al. 2002, Terashima et al. 2005). If this is valid, it is expected that shoot growth of MBs would be suppressed. However, in the present study, the shoot elongation was suppressed more in CBs than in MBs in 2002 (Table 2-1). It is highly probable that this tendency is due to that I chose branches with higher priority (i.e., leader branches) as the MBs. Then, the relative sink strength due to shoot elongation would be stronger in MBs than in CBs, because shoot elongation was affected not only by its light environment and but also by its relative priority such as relative stem thickness (Goulet et al. 2000, Nikinmaa et al. 2003) or branch order (Suzuki 2002, 2003).

Interestingly, effects of the manipulations of MBs were also observed in CBs (Table 2-1, Figure 2-3). Similar changes in A/N_f and in the branch diameter growth were found in CBs (Figures 2-4, 2-5, 2-7). These indicate that the decrease in the total

photosynthetic production of a tree individual affected the diameter growth of CBs. In this context, the branch autonomy principle does not suggest anything. Instead, the sink-source balance would be a very important determinant of the diameter growth pattern. The photosynthates produced in a given branch are used not only for its own growth and respiration but also for those of the downstream organs such as branches, trunks and the root systems. When photosynthetic production in the MBs was suppressed, growth of MBs was reduced and that used in the downstream organs would be also reduced. Instead of the MBs, photosynthetic production of which was suppressed, the CBs needed to contribute much more proportion of their photosynthates to the maintenance of the downstream organs than that would be without the manipulation of MBs (Figure 2-8). Then, the diameter growth and the shoot elongation would be suppressed in CBs. This compensating mechanism would make the difference in A/N_f between MBs and CBs smaller and contribute to maintenance of the pipe-model relationships. The importance of these compensating mechanisms has not been pointed out so far.

Effects of the previous-year conditions or hysteresis are very important. In the next year of the manipulations, the increase in the leaf number and the proportion of long-shoots were suppressed in both CBs and MBs. Not only the shoot elongation but also the diameter growth may depend at least partly on the photosynthetic production in the previous year. The suppression of shoot elongation causes suppression of leaf increment, thereby, the demand for photosynthates to the branch diameter growth would be suppressed. Therefore, both of the important determinants, the demand for and supply of photosynthates, of the branch diameter growth are suppressed. In this way, the previous-year conditions and the production can affect branch growth in the next year, and contribute to stabilization of the pipe-model relationship (Figure 2-8).

The pipe-model relationship is stabilized more by the control of the leaf amount rather than that of the branch diameter growth. This is probably because the leaf amount is easier to control than the branch cross-sectional area that in previous year is already determined. In addition, the branch diameter growth that is limited by photosynthetic production is not able to increase so large. What are the control mechanisms? The pipe-model relationship was altered when the light intensity or the leaf amount in MBs was suppressed. In these situations, the supply of photosynthates in MBs would be

smaller than the demand (i.e., shoot elongation in MBs was little suppressed in the current-year). The increase in the leaf amount and shoot elongation would depend on the photosynthetic production in the previous year. Therefore, leaf amount and shoot elongation suppressed in the next year in both MBs and CBs by sharing the stored photosynthates among branches. Then, the imbalance would be compensated and the pipe-model relationship would be recovered. This compensation is caused by suppression of supply (leaf amount) of photosynthates, accompanied by suppression of demand (shoot elongation) of those, for the branch growth.

The study described in Chapter 1 clarified the significance of 'branch priority' for the branch diameter growth (Sone et al. 2005, Terashima et al. 2005). The regulation mechanisms found in the present study differs from the concepts of 'branch autonomy' and 'branch priority' and may be called 'branch cooperativeness.' Construction and maintenance of the pipe-model architecture would be regulated by the balance between priority and cooperativeness among branches.

Table 2-1. Changes in leaf number, branch cross-sectional area and proportion of long shoot. For control tree, leaf number and long shoot proportion are shown for a tree individual, and branch cross-sectional area is for main stem at the crown base. For manipulated trees, these data were shown for control (CBs) and manipulated (MBs) brabches, respectively.

	Leaf number			Branch cross-sectional area (mm2)			Long shoot proportion (%)		
	2001	2002	2003	2001	2002	2003	2001	2002	2003
Control tree	1188	1596	1868	1762	2124	2734	5.3	10.0	8.9
Shade									
CBs	78	130	144	196	210	221	14.3	7.8	10.6
MBs	391	584	534	629	699	748	7.3	14.4	4.7
Half cut									
CBs	419	644	600	649	1025	1231	14.5	10.2	5.5
MBs	218	348	294	315	393	473	19.4	7.4	0
Half pick									
CBs	184	206	98	212	296	316	15.2	13.3	8.9
MBs	126	147	248	169	222	268	18.9	24.3	13.1
Long shoot pick									
CBs	926	1200	667	1025	1465	1795	8.0	6.6	2.8
MBs	820	964	1222	560	822	1127	16.5	0	9.8

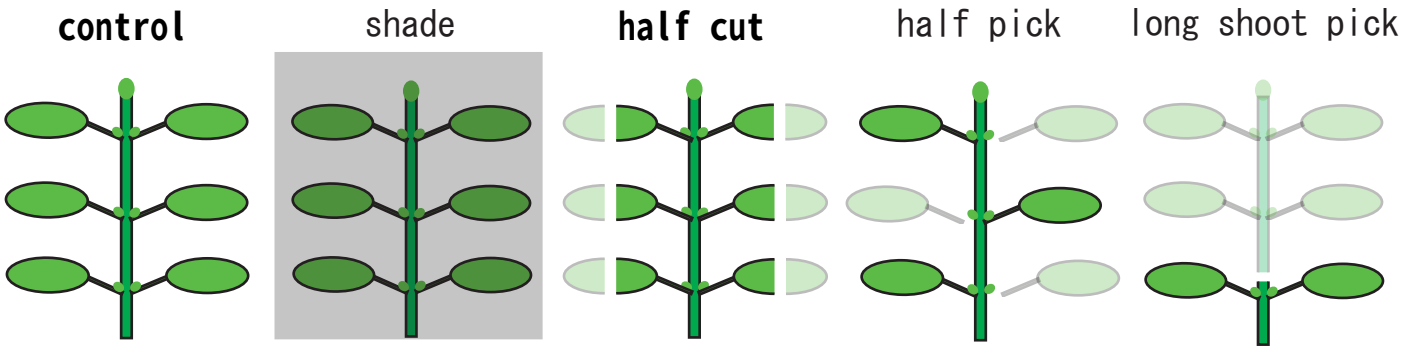

Figure 2-1. Diagrams of branch manipulations. Current-year long shoots are shown for simplicity. Short shoots had only two leaves. All current-year shoots including both long and short shoots within the branch were manipulated in manipulated branches (MBs). Growth light intensity was decreased to 15% with shade manipulation. Half cut and half pick manipulations were conducted for all leaves within MBs. In the half cut manipulation, the leaf area was decreased to the half, but the leaf number did not change. The half pick manipulation was conducted by removing leaves alternately, and leaf number and area were decreased to the half. By long-shoot pick manipulation, all current-year shoots had only two leaves like short shoots. This manipulation restricted both shoot elongation and leaf increment.

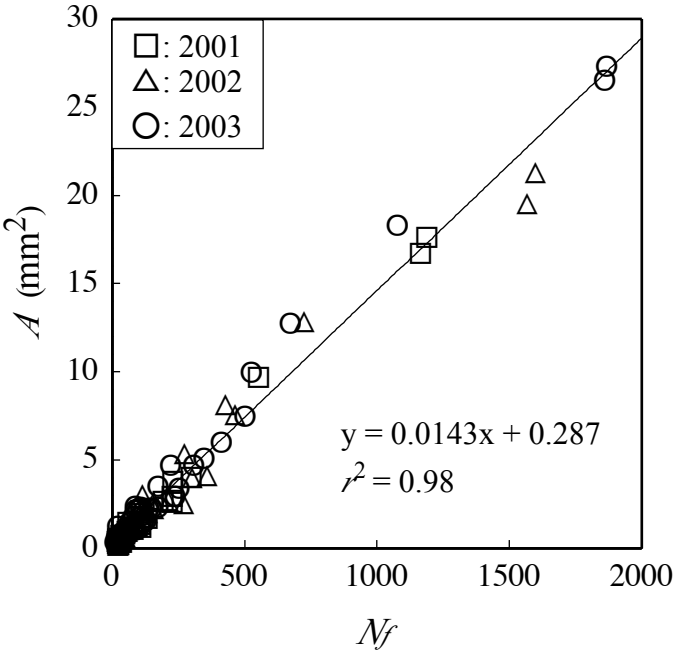

Figure 2-2. Relationship between branch cross-sectional area (*A*) and leaf number for the branch (*Nf*) within the crown of the control tree. Symbols: □ = 2001; △ = 2002; and ○ = 2003. The regression line was drawn with the data for all year.

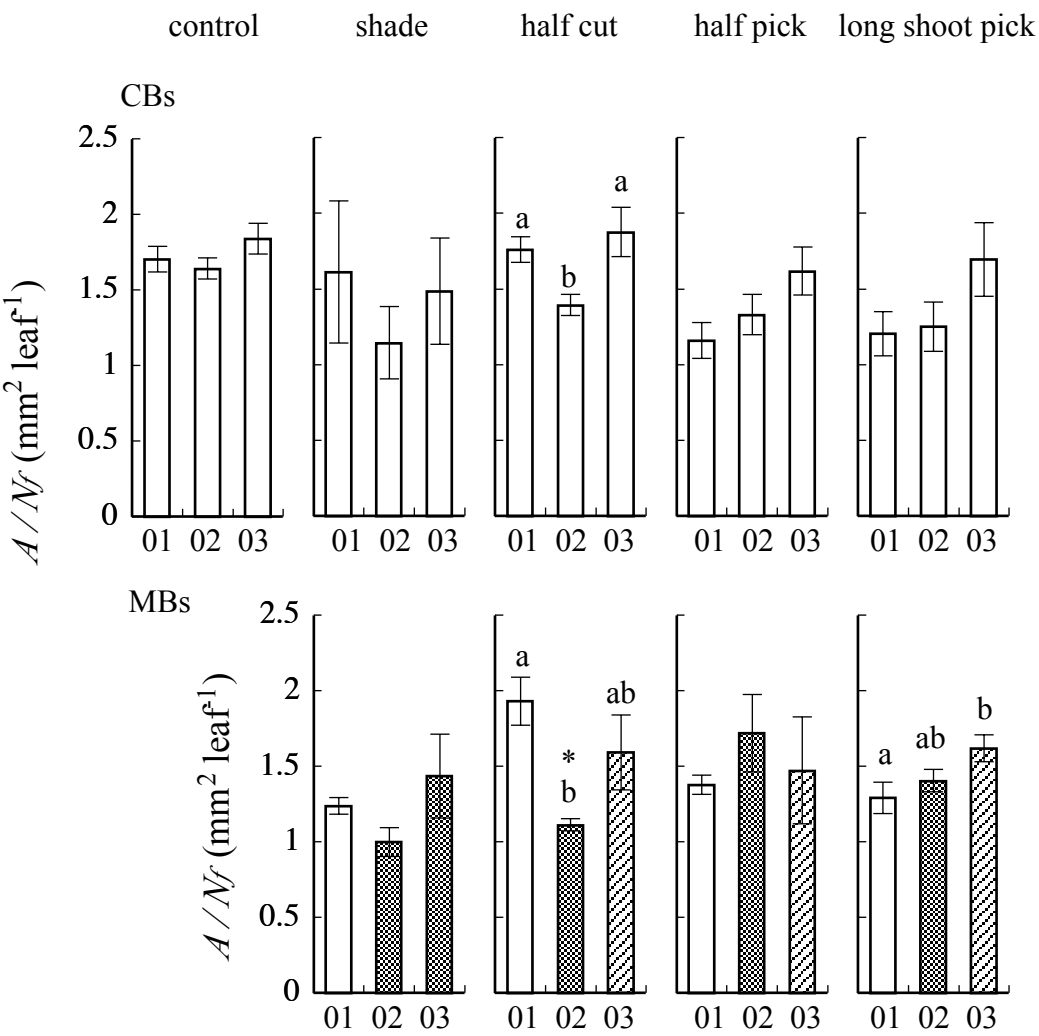

Figure 2-3. Changes in the ratio of branch cross-sectional area to leaf number of the branch (*A*/*Nf*). The data of the control tree (CT) and control branches (CBs) in manipulated trees (MTs) are shown in the upper panels. In lower panels, the data of manipulated branches (MBs) in MTs are shown. Open, dotted and hatched bars denote the data of MBs in the year of control, that of manipulation and untreated MBs that were manipulated in the previous year (MBs), respectively. Different letters mean significant difference among years ($p < 0.05$, Tukey-Kramer's test). * indicates significant difference between CBs and MBs ($p < 0.05$, Student's t test). Error bars are mean ± S.E.

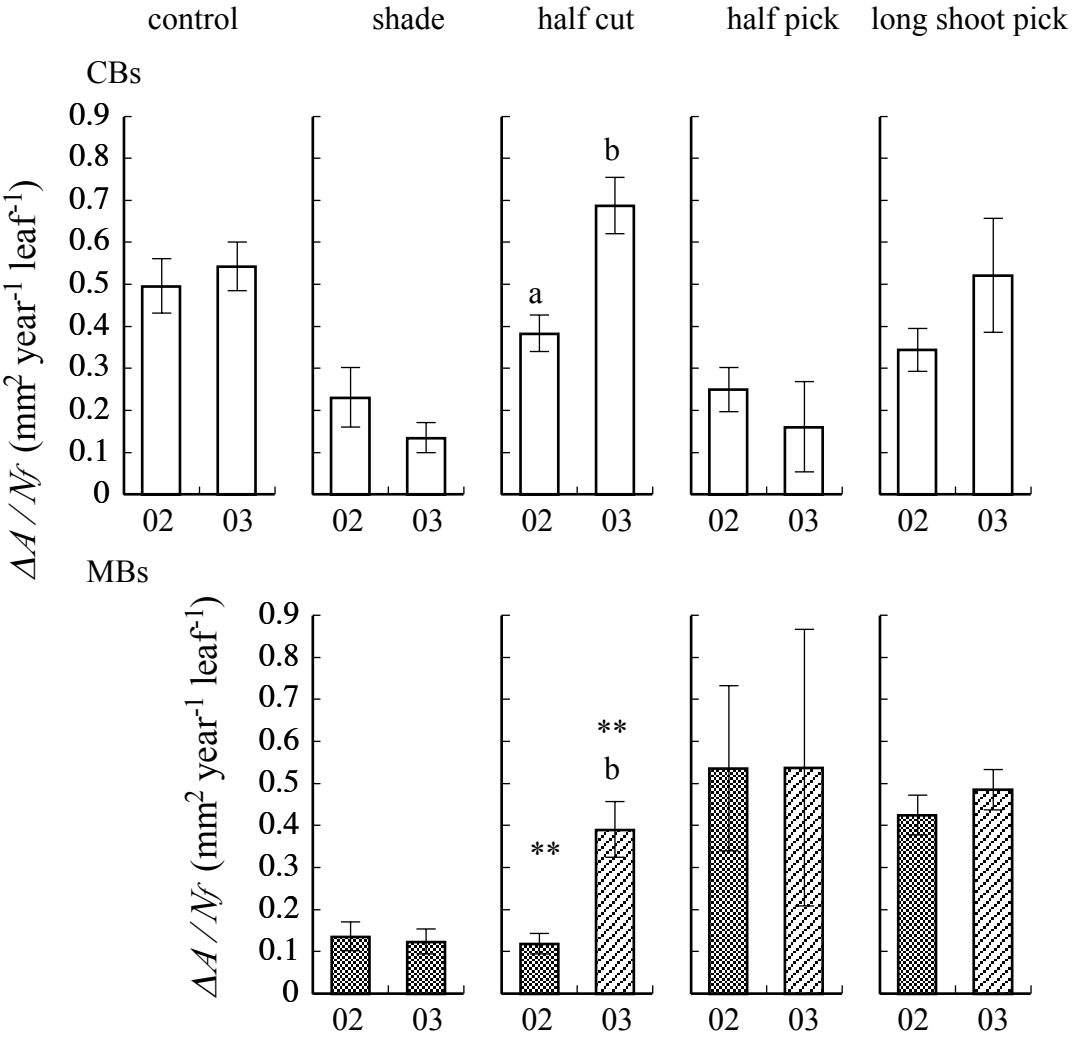

Figure 2-4. Changes in the ratio of yearly growth of branch cross-sectional area to leaf number ($\Delta A/Nf$). The data of the control tree (CT) and control branches (CBs) in manipulated trees (MTs) are shown in the upper panels. In lower panels, the data of manipulated branches (MBs) in MTs are shown. Dotted and hatched bars denote the data of MBs in the year of manipulation and untreated MBs that were manipulated in the previous year (MBs), respectively. Different letters mean significant difference among years ($p < 0.05$, Tukey-Kramer's test). ** indicates significant difference between CBs and MBs ($p < 0.01$, Student's t test). Error bars are mean ± S.E.

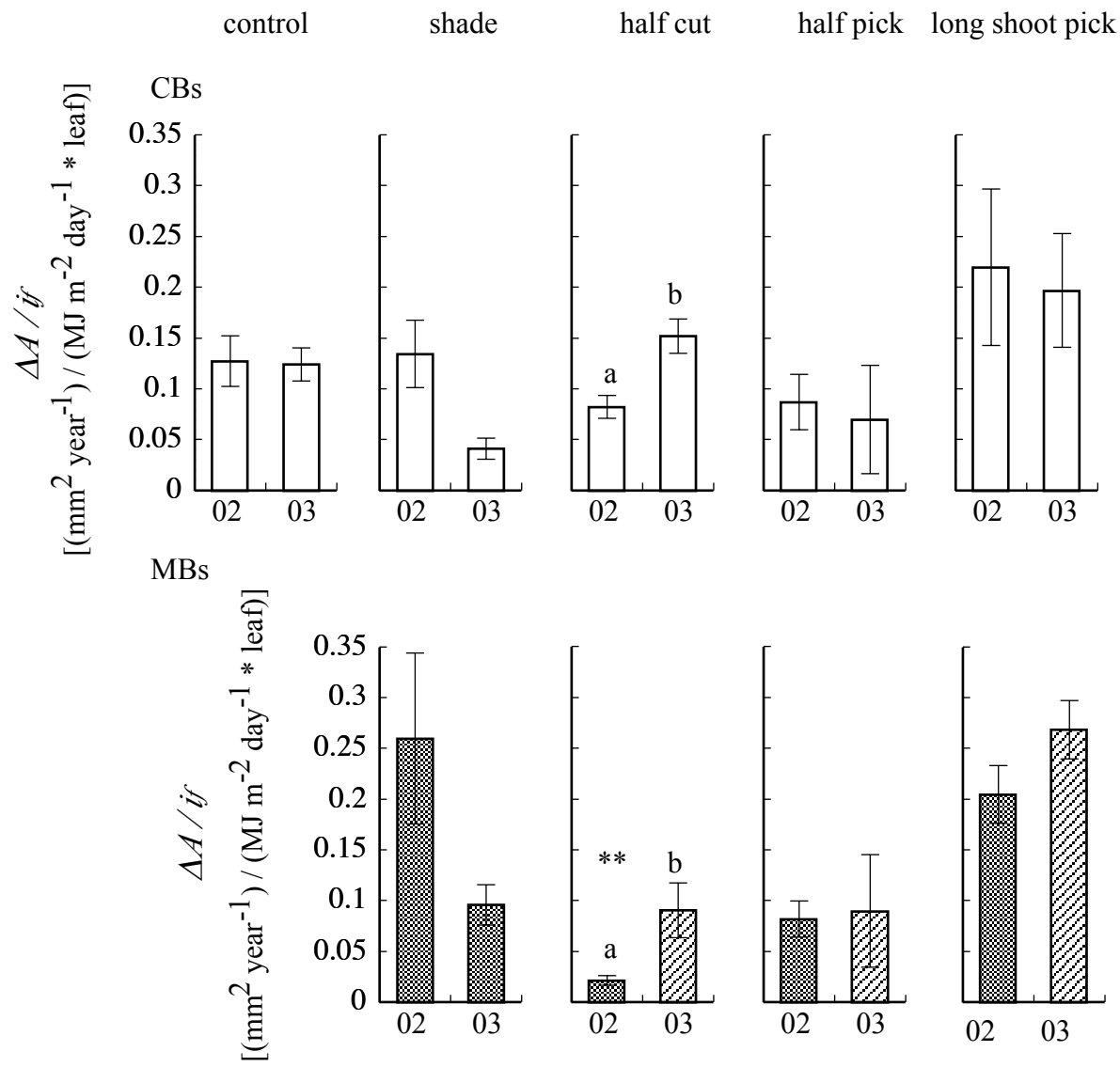

Figure 2-5. Chantes in the ratio of yearly growth of branch cross-sectional area to light interception (*ΔA/if*). Bars are the same with Figure 2-4. Different letters mean significant difference among years ($p < 0.05$, Tukey-Kramer's test). ** indicates significant difference between between CBs and MBs ($p < 0.01$, Student's t test). Error bars are mean ± S.E.

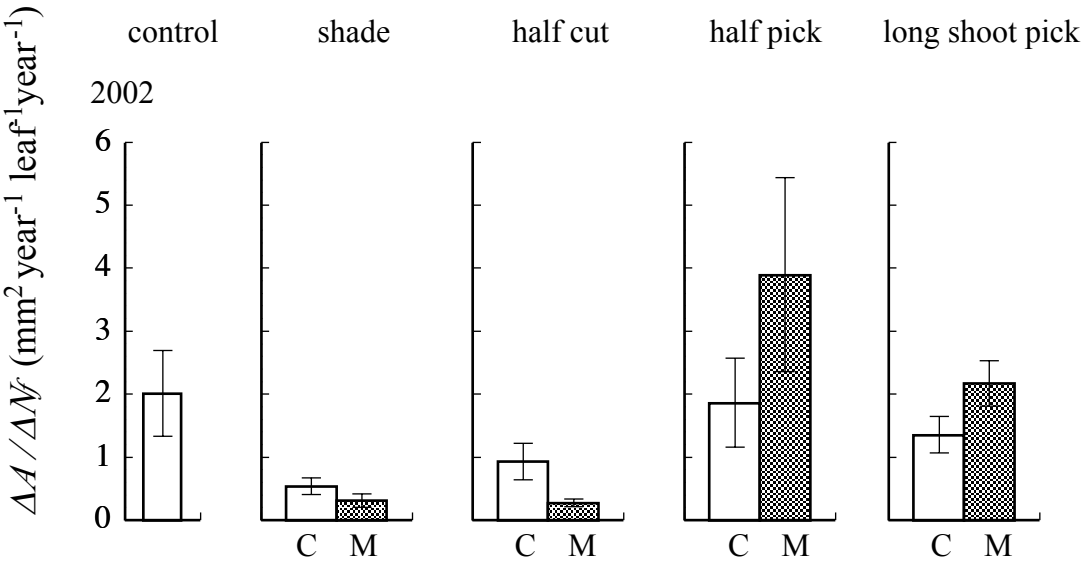

Figure 2-6. Changes in the ratio of the yearly growth of branch cross-sectional area to yearly increment of leaf number ($\Delta A/\Delta Nf$). Open and dot bars are control (C) and manipulated (M) branches, respectively. Error bars are mean ± S.E.

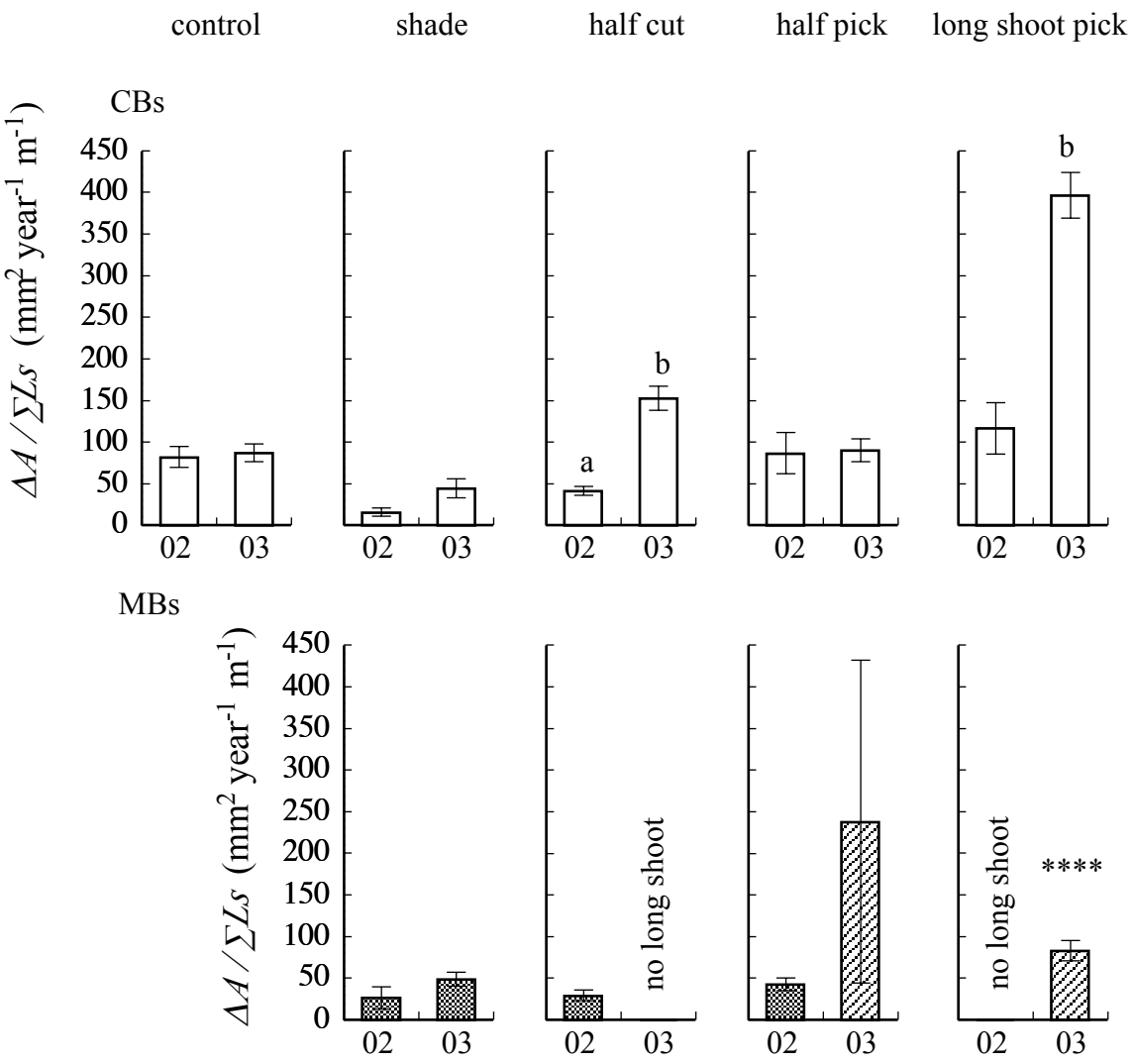

Figure 2-7. Changes in the ratio of yearly growth of branch cross-sectional area to sum of long shoot length ($\Delta A/\sum Ls$). Bars are the same with Figure 2-4. Different letters mean significant difference among years ($p < 0.05$, Tukey-Kramer's test). **** indicates significant difference between CBs and MBs ($p < 0.0001$, Student's t test). Error bars are mean ± S.E.

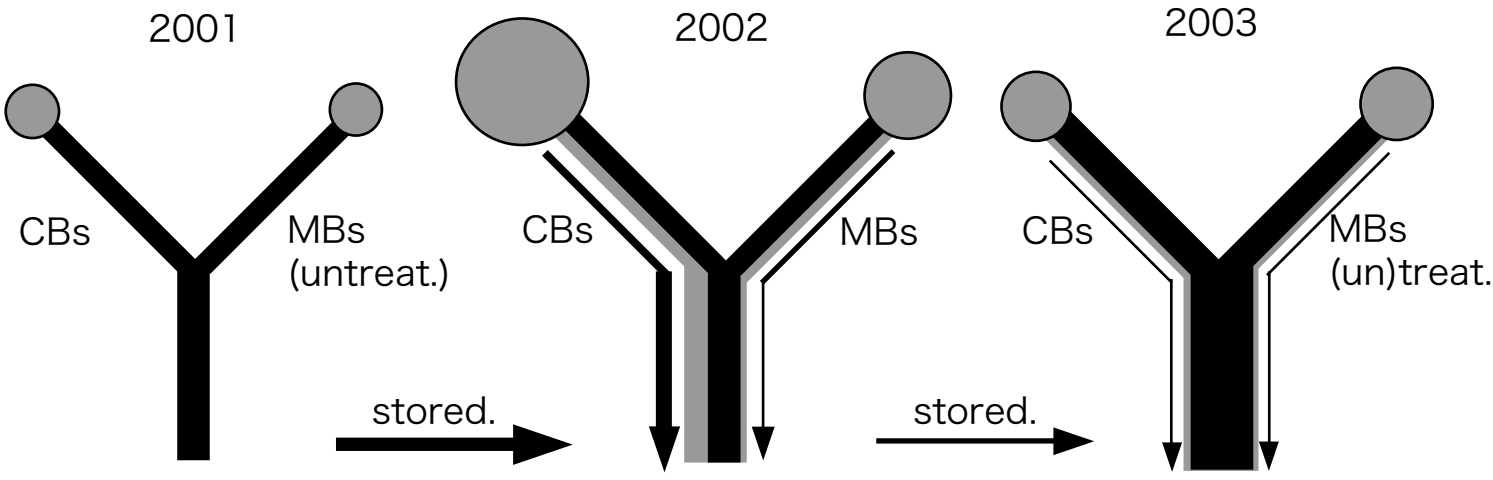

Figure 2-8. A model for diameter growth of the branches and trunks and allocation of photosynthates. Left and right branches are control (CBs) and manipulated (MBs) branches, respectively. Areas of circles indicate leaf amount or light interception of the branch. Shaded parts of the stems indicate the wood produced in the current year. Solid parts of the stems denote the wood existed in the previous year. Thickness of arrows indicate amount of the photosynthate translocation.

(Chapter 3)

Mechanical and ecophysiological significance of young *Acer* tree design: Vertical differences in mechanical properties and xylem anatomy of branches

Introduction

To understand tree design, we should consider mechanical factors. It is obvious that stems should be tough enough to support themselves and their leaves under gravitational, windy, rainy and/or snowy conditions.

Shinozaki et al. (1964*a*, *b*) found that, for any branch within a tree crown, there is a proportional relationship between the cumulated leaf mass for the branch and its basal cross-sectional area. This strong relationship led them to propose the pipe-model theory. The proportionality, however, does not hold for the trunk below the crown. Oohata and Shinozaki (1979) found that dry mass of a branch with its leaves is proportional to its basal cross-sectional area. Assuming that the load of the biomass always applies to the stem cross-section vertically, they proposed that the compressive stress at any position of the stem within the tree is constant. Then, the tapering of the trunk below the crown was explained. However, actual loads of branches are not necessarily normal to their cross-sections, because the branches variously incline.

Based on theories of mechanics, Greenhill (1881) calculated the critical buckling height of the tapering pole. Using the Greenhill's formula, McMahon (1973) computed the critical buckling height of the tree. Assuming that the ratio of elastic modulus (E) to density (ρ) of the material is constant, McMahon (1973) claimed that the critical buckling height of the tree is proportional to 2/3 power of the basal diameter of the trunk (D_T). McMahon and Kronauer (1976) further regarded the branches as tapering

cantilever beams that have the same inclination and are composed of a uniform material. Then, the branch length (L_B) is also proportional to 2/3 power of the basal diameter of the branch (D_B): $L_B \propto D_B^{2/3}$. Such the scaling relationship is called the elastic similarity model (McMahon 1973, McMahon and Kronauer 1976). McMahon and Kronauer (1976) also proposed the constant stress model, in which the maximal stress of the branch due to the bending moment caused by its own weight is constant when $L_B \propto D_B^{1/2}$. Other models such as the geometric similarity model ($L_B \propto D_B$) (McMahon and Kronauer 1976, Norberg 1988, Bertram 1989, Niklas 1992, 1994) and the constant wind stress model ($L_B \propto D_B$) (King and Loucks 1978, King 1986, Speck et al. 1990) have been also proposed. These mechanical models have been used in many studies to argue significance of the tree architecture (King and Loucks 1978, Dean and Long 1986, King 1986, Norberg 1988, Bertram 1989, Niklas 1992, 1994, Suzuki and Hiura 2000). In several studies, the tree architecture was analyzed from the viewpoints of both biomechanics and water conduction (Mencuccini et al. 1997, West et al. 1999, Berthier et al. 2001, Taneda and Tateno 2004).

Most of these mechanical models assume that trees and branches within a tree have the same mechanical properties. However, this assumption is invalid. It is therefore important to take into account the variations in branching angle or stem inclination (Murray 1927) and in the mechanical property among tissues (Niklas 1992, 1994) and among branches (Bertram 1989, Niklas 1997, Mencuccini et al. 1997). Also, mechanical stress of the branches would be different within the tree. Morgan and Cannell (1994) indicated that the stress distribution within a main trunk changes depending on wind speed. Chiba (2000) suggested that, in plantation forests of conifer species, the trunk position receiving the maximal stress shifts downward from crown base to trunk base until the diameter at breast height of the tree attains 15-20 cm, and then, the position again shifts upward to the crown base. He also showed that the positions receiving the maximal stresses almost accorded with the positions where the trees were snapped by typhoons. Therefore, it is necessary to examine the actual mechanical status in various parts (Tateno and Bae 1990).

Branches within an asymmetric crown develop in such a way that reduces the bending moment of the tree trunk. Formation of the reaction wood also ameliorates imbalance in the mechanical stress (Mattech and Kubler 1995). In spite of these effects,

heterogeneity in the mechanical status among the branches within a tree can be very large. For example, branches at lower positions would not suffer mechanical stresses caused by strong winds, while the upper branches are often blown by strong winds. Another point is that lower branches in shaded environments tend to incline more horizontally than upper branches. Such horizontal orientation of the lower branches is effective not only in increasing light interception by evenly displaying shade leaves but also in saving cost of the mechanical support in such branches (Cannell et al. 1988, Morgan and Cannell 1988). Moreover, if such the lower branches have shorter residual longevity than the upper branches, the cost can be further saved by reducing mechanical safety. Therefore, vertical differences in the mechanical status of the branches would be very important for adaptive significance of the mechanical tree design.

In this study, I measured the actual branch dimensions such as inclination, height, fresh weight, length, length of lever arm, foliage-cluster position, growth ring thickness, long shoot proportion, etc. of 49 branches in two 10-year-old *Acer rufinerve* trees of 3.0 and 5.4 m in height. I also measured the elastic modulus in 29 branches. Moreover, I examined anatomy of cross sections of nine branches, and quantified the area density of fiber cell walls and the cell wall thickness of the fiber. Using these data, I calculated the bending moment, compressive force, section modulus, second moment of area, flexural stiffness, stress, and curvature of deflection of the branch. Based on these measurements and calculations, I analyzed differences in the mechanical properties and growth of the branches within the tree. Mechanical and eco-physiological significances of the tree design are discussed.

Materials and methods

Study site and species

Two 10-year-old *Acer rufinerve* (Siebold et Zucc.) trees of 3.0 and 5.4 m in height were analyzed. These trees were in the Ashu Experimental Forest of Kyoto University, Kyoto, Japan (35˚20’ N, 135˚45’ E, 700 m a.s.l.), where mean annual temperature and precipitation for the last 10 years were 12.3˚C and 2400 mm, respectively. *A. rufinerve* is a deciduous, broad-leaved and semi shade-tolerant. At maturity, the trees often reach the forest canopy. The phyllotaxis is decussate and the branching pattern is monopodial

(Sakai 1990). Leaf expansion and secondary growth of stems started in early May. Secondary growth finished in early September (Komiyama et al. 1987, 1989).

Measurement of branch dimensions

The measurements were conducted in August 2001 with one tree (H = 5.4 m) and in November 2002 with another tree (H = 3.0 m). At sampling, one tree (H = 5.4 m) had green leaves and the other (H = 3.0 m) had shed all the leaves. Measurements of several branch characteristics (see below) were carried out in the field.

A tree can be generally regarded as a fractal-like architecture. These sample trees had 33 (with leaves, H = 5.4 m) and 16 (without leaves, H = 3.0 m) main branches of various sizes, respectively. Large branches included smaller branches within them, and thus, the largest branches were the tree-individuals themselves. For each branch, inclination of the axis from the vertical (θ), length (L_B), diameter at the base (D_B), distance from the tree top level to the branch base (d_{BB}), distance from tree top to the center of the leaf cluster (d_{LC}), and the number of long shoots relative to the total number of current-year shoots (L/T) were measured (Figure 3-1, A). I defined the long shoots as those having four (two pairs) or more leaves. The shoots having two leaves (one pair) were regarded as short shoots (data not shown). There are two reasons for this definition. 1) All the winter buds of this species have two leaves and 2) internodes of the shoots having four or more leaves were markedly longer than those of the shoots having two leaves (data not shown). D_B was measured in vertical (D_{BV}) and horizontal (D_{BH}) directions. After these measurements, the trees were cut.

For each branch, the branch age (α) was determined through counting number of annual rings with its cross-section at the base. As an index of cross-sectional growth, the average space between annual rings ($\Delta_{AR} = 0.5\ D_B/\alpha$) was calculated. I measured the branch fresh-mass (m; including leaves, when present) with a spring balance at the center of gravity (Figure 3-1, B). Length from the center of gravity to the branch base (L_{LA}) was also measured. I regarded L_{LA} as length of the lever arm.

Calculation of bending moment and stress

I calculated gravitational force of branch mass (F_M) of each branch and F_M was divided into two force components (Figure 3-1, A). One was compressive force (F_C) that

paralleled the axis of the branch. The other was bending force (F_B) that was perpendicular to the axis:

$F_M = m\,g$ (3-1),

$F_C = F_M \cos\theta$ (3-2),

and

$F_B = F_M \sin\theta$ (3-3),

where g is acceleration of gravity. In addition, bending moment (M) was calculated from eqn. (3-3):

$M = F_B\,L_{LA.}$. (3-4),

Cross-sectional area (A_B), section modulus (Z) and second moment of area (I) of the branch were calculated as (Figure 3-2, A):

$A_B = \pi\,D_{BV}\,D_{BH} / 4$ (3-5),

$Z = \pi\,D_{BV}^2\,D_{BH} / 32$ (3-6),

and

$I = \pi\,D_{BV}^3\,D_{BH} / 64$. (3-7)

Z has the dimension of the cube of length and I has that of the fourth power of length. From the compressive force (F_C), bending moment (M), cross-sectional area (A_B) and section modulus (Z), I calculated the stress (σ). Bending stress of the branch due to the bending moment generated by the weight-force of the branch is largest at the uppermost and lowermost parts within the cross-section. On the other hand, compressive stress of the branch due to the compressive force is uniform within the cross-section. The maximal bending stress (σ_{max}) and the compressive stress (σ_C) were

$\sigma_{max} = M / Z,$ (3-8)

and

$\sigma_C = F_C / A_B$, (3-9),

respectively. The total stress (σ) was calculated as $\sigma_{max} + \sigma_C$. Therefore, σ was the maximal stress within the cross-section. In practice, σ was approximately equal to σ_{max} ($\sigma \approx \sigma_{max}$), because σ_{max} was larger by two orders of magnitude than σ_C.

Determination of elastic modulus

Elastic modulus (E) was determined for 29 branches out of 49 branches. These 29 branches had straight stems. E was determined by measuring bending of the branch (Figure 3-2, B). I used fresh branch samples with their barks. The most basal part of the sample branch was suspended horizontally on two edges and loaded with force (F) at the midpoint between the edges with a spring balance. I applied various loads and measured the corresponding deflections (δ) at the midpoint. The load was varied within the elastic range. E was calculated as

$E = (F L_S^3) / (48 I \delta)$ (3-10),

where Ls was the distance between the two edges. In this calculation, the second moment of area (I) used was the mean of three cross-sections measured at the distal (I_d), middle (I_m) and basal (I_b) positions between the two edges in the branch (Figure 3-2, B). After this measurement, the sample of about 1 cm thickness was cut from the basal end of the branch and dried at 80˚C for 3 days. The dried samples were weighed and their volumes were measured. From these, density of the sample (ρ) was determined.

Calculation of curvature

E is rigidity determined by the material and I is bending rigidity determined by the size and shape of the cross section. Therefore, flexural stiffness (EI) increases with E and/or I. There is a relationship between the bending moment (M) and the flexural stiffness (EI) expressed as:

$M = (1/R) EI$ (3-11)

where, R is the radius of curvature of the branch deflection, and thus $1/R$ is curvature of the deflection.

Measurement of xylem anatomy

Xylem anatomy was examined in nine branches from both trees. The samples about 1 cm thickness, from the branch base, were sliced with a razor blade and were observed under a microscope (BX50, Olympus, Tokyo). I took digital images of the current-year xylem with a digital camera (C-3040, Olympus). In two samples of the main trunks at the crown bases of the two trees, images of xylem were taken for the respective growth rings (10-year). Fiber cell walls, vessels and rays were traced on the digital images using the software, Adobe Photoshop CS (Adobe Systems Incorporated, California, U.S.A.), and measured their areas with the NIH-Image v. 1.63 software (US National Institutes of Health). The area occupied by fiber cell walls relative to unit xylem area (A_{FW}, fiber cell wall density; %) was calculated. The average fiber cell wall thickness (T_{FW}) was calculated as:

$$R_{FW} = A_{FW} / A_{FT} \qquad (3\text{-}12),$$

$$A_{FC} = A_{FT} / N_{FC} \qquad (3\text{-}13),$$

and

$$T_{FW} = (A_{FC} / \pi)^{1/2} - \{ A_{FC} (1 - R_{FW}) / \pi \}^{1/2} \qquad (3\text{-}14),$$

where, R_{FW} , A_{FT}, A_{FC}, and N_{FC}, are area occupied by fiber cell walls per unit fiber tissue area, area occupied by fiber tissue per unit xylem area, average cross sectional area of a fiber cell, and fiber cell number per unit xylem, respectively. In eqn. (3-14), cross-section of a fiber cell was regarded as circle.

Statistical analyses

Linear, power and multiple regression analyses were performed using software (Stat View J-5, SAS Institute, Inc., North Carolina, U.S.A.).

Results

Elastic modulus

In many studies, elastic modulus (E) is correlated with wood density (ρ) (Niklas, 1994). In this study, however, E was not correlated with ρ (r = 0.204, p > 0.05; data not shown). Instead, E was correlated with depth from the tree top level to the branch base (d_{BB}), branch length (L_B), stress (σ), and branch inclination (θ) (Table 3-1). Using a multiple regression analysis, the elastic modulus was expressed as:

$$E = 4.504 - 2.595 d_{BB} + 0.993 L_B + 2.374 * 10^{-7} \sigma + 0.023 \theta \qquad (3\text{-}15).$$

Thus, E mainly depended on d_{BB} among four parameters (Table 3-1). The lower branches tended to show lower E (Figure 3-3).

Using eqn. (3-15), I calculated E of the branches whose E were not measured because they were not straight. E thus estimated were used for the calculation of the flexural stiffness (EI) for such branches.

Stress and curvature

σ increased with the depth of branch base from the crown top (d_{BB}) (Figure 3-4 – upper left). The tendencies, however, were different between branches forming the main trunk (main stems) and lateral branches, in particular when the tree had leaves. The increment was steeper in the laterals than the branches that formed the main trunk. This difference was not found in the relationship between σ and the depth to the leaf cluster (d_{LC}) (Figure 3-4 – upper right). This is because the main stems inclined little so that their leaves were at higher positions than those of the lateral branches with similar d_{BB}. There was a clear tendency that the stems having the leaves at higher positions received lower stress.

The radius of curvature of the branch deflection (R) decreased with the increase in d_{BB} or d_{LC} (Figure 3-4 - lower). This means that the lower branches showed the larger deflections than upper branches. Similarly, to the pattern for the stress, the main stems had smaller curvature (larger R) than laterals. This difference between branch groups was not found in the relationship between R and d_{LC}.

σ and R also depended on the growth activity such as the long shoot proportion (L/T) and the average thickness between annual rings (Δ_{AR}) (Figure 3-5). σ was small

and R was large for vigorous branches within the tree. When the branches had leaves, σ were larger and R were smaller.

σ and R were also correlated with the branch inclination (θ) (σ, $r = 0.465$, $p < 0.001$ and R, $r = -0.337$, $p < 0.05$, respectively), but not with length (L_B) (σ, $r = 0.013$, $p > 0.05$, R, $r = 0.197$, $p > 0.05$) or age (α) (σ, $r = 0.140$, $p > 0.05$, R; $r = -0.110$, $p > 0.05$) of the branch (data not shown).

Xylem anatomy

Proportions of areas of the fiber tissue, vessels and rays per unit xylem area did not change irrespective of stem position and of xylem age. The proportions of fiber tissue, vessels and rays were about 80%, 10% and 10%, respectively (data not shown). The bending stress increases toward the radial direction and thus should be maximal at the current-year xylem. The elastic modulus (E) of the branch increased with the increase in the fiber cell wall density (A_{FW}; area occupied by fiber cell walls per unit xylem area) and/or that in the average fiber cell wall thickness (T_{FW}) of the current-year xylem (Figure 3-6).

A_{FW} of the current-year xylem slightly decreased with the increase in d_{BB}, although the relationship was not significant ($r^2 = 0.36$, $p = 0.09$) (Figure 3-7). T_{FW} of the current-year xylem did not depend on d_{BB}.

Examination of the cross section of the trunks at the crown bases revealed that T_{FW} tended to be thinner in the inner xylem (i.e. older xylem). On the other hand, A_{FW} was independent of xylem age. Interestingly, A_{FW} and T_{FW} oscillated with the period of 2 or 3 years (Figure 3-8).

Discussion

Variations in elastic modulus and xylem anatomy within the tree

My results with *A. rufinerve* trees clearly showed that the mechanical properties of the branches varied greatly. E differed considerably among branches (Table 3-1 and Figure 3-3). E increased with σ and/or θ (Table 3-1). This means that the stress and gravity affect stiffness of the stems (Mattech and Kubler 1995). However, d_{BB} affected E more strongly than σ or θ.

Niklas (1997) indicated the heterogeneity of E within a 43-year-old black locust (*Robinia pseudoacacia* L.). In his study, E increased with increase in the stem age and length, and the inner xylem of heartwood was stiffer than the outer xylem. Inversely, Mencuccini et al. (1997) indicated that outer xylem was stiffer than inner xylem in Scots pine (*Pinus sylvestris* L.). In *Cryptomeria japonica* (L.f.) D. Don, the outer xylem is stiffer than the inner xylem, and the outer and inner xylems are called mature and immature wood, respectively (Fushitani 1985). The fiber cell length and wall thickness are greater in outer xylem than those in the inner xylem, inclination angle of cellulose micro-fibril of outer xylem is smaller (more vertical) than that in inner xylem, and crystallinity of the cellulose is higher in outer xylem than that in inner xylem (Fushitani 1985).

In the present study, E decreased with d_{BB} (Figure 3-3). E also increased with the increment of A_{FW} and T_{FW} of the current-year xylem (Figure 3-6). In the current-year xylem, A_{FW} was slightly denser in upper branches than in lower stems, but T_{FW} did not depend on d_{BB} (Figure 3-7). On the other hand, in the main trunk at the crown base, the inner and older xylem had smaller T_{FW} than the outer and younger xylem, although the A_{FW} was independent of age (Figure 3-8). These results indicate that the lower and older branches are softer than the upper and younger branches, because A_{FW} of the current-year xylem (most peripheral part) was smaller in lower branches, and T_{FW} is thinner in inner and older xylem. It was also suggested that, within the cross-section, young and peripheral parts were stiffer. Because the stress due to bending moment is greater in more peripheral parts, this radial gradient in stiffness would be efficient (Figure 3-9).

Mechanical and ecophysiological implications of the tree design

σ and R depended on the branch position and vigor (Figures 3-4 and 3-5). Increments of σ and decrement of R with depth to the branch base (d_{BB}) differed between the main stems and lateral branches (Figure 3-4 - left). In the lateral branches, the increase in σ and decrease in R with d_{BB} were steeper than those in the main stems, while there were no differences between σ or R and the depth to the leaf cluster, d_{LC} (Figure 3-4 - right). This reflected that the inclinations of the main stems were smaller than those of the lateral branches, and that the main stems had their leaves at upper positions. Stems

(including main stems and lateral branches) having leaves in the upper and brighter positions were subject to smaller stress and curvature than those in lower and shaded positions. This is reasonable because promising and productive branches at upper positions are mechanically safer than the lateral branches at lower positions, which are unproductive and having shorter residual longevities.

In a previous study (Chaper 1), I found that, in *A. rufinerve* used in this study, the rate of branch diameter growth was determined by two factors, light interception and shoot elongation rate of the branch (Sone et al. 2005, see also Terashima et al 2005). This result suggested that the branch diameter growth depend not only on its photosynthetic production but also on its relative priority among the branches. σ and R also depended on the growth activity (Figure 3-5). Thus branches having high growth rate in diameter and in length were constructed so as to be mechanically safer. The results in Chapter 1 already indicated that the stress and deflection would be smaller in vigorously growing branches. This is because the stem diameter strongly affects the second moment of area (I) and section modulus (Z). Also, in the branches with low growth rates, E would be smaller, because inner and older xylem had thinner T_{FW}. Thus, flexural stiffness (EI) and Z was greater in upper, younger, productive and promising stems that showed smaller stress and deflections. On the other hand, the lower branches had smaller EI and Z, thereby, had greater stress and curvature. The reduced investment to the diameter growth of the lower branches is adaptive from a viewpoint that the lower unproductive branches will die back soon. The difference in the curvature between upper and lower branches indicates that lateral branches would gradually incline with aging and/or height growth of the tree (Figure 3-9).

Tree design for production and growth

R was greater in the stems of the tree without leaves than those with leaves condition (Figure 3-5). The large difference would be attributed to presence of leaves, because leaves comprise a considerable part of the branch mass, in particular thin branches.

In *A. rufinerve*, the secondary growth starts with the shoot extension in spring (Komiyama et al. 1987, 1989). This growth phenology suggests that the branch deflection occurring in spring due to leaf expansion was gradually recovered with the increase in I due to the diameter growth of the stem. The stems with greater annual ring

thickness (Δ_{AR}) and long shoot proportion (L/T) showed greater R (Figure 3-5). In stems with greater Δ_{AR} and L/T, the recovery of deflection should be most prominent. Consequently, the vigorous and promising stems would be lifted more vertically and show decreased stress and curvature. On the other hand, in the stems with smaller Δ_{AR} and L/T, the recovery of deflection would be imperfect, because of small investment to the diameter growth in such branches (Cannell et al. 1988, Morgan and Cannell 1988). Low diameter growth rate and aging cause low flexural stiffness (EI). Consequently, the lower branches would gradually become horizontal and subject to the greater stress and curvature. However, the lower branches tend to develop lateral shoots rather than to elongate (i.e., weaker apical dominance and thereby reducing the length of lever arm). The morphology of the lower branches would be efficient in reducing the bending moment generated by their own weights.

Leaves can acclimate to their own light environments and differentiate sun and shade leaves (Björkman 1981). Inclinations of the leaves and shoots also differ depending on their light environments (Kikuzawa 1995, Kikuzawa et al. 1996). Not only small inclinations of the leaves and the shoots, but also the vertical orientations of the upper branches would be effective in letting the excess light transmit to the lower branches, because projected leaf areas of such branches are small. On the other hand, lower horizontal branches are suitable for displaying their less inclined shade leaves to increase light interception by avoiding mutual shading. In addition, the lower branches would be effective for increasing the projection area of the tree crown. Efficient light interception for the whole tree-individual would be thus realized (Figure 3-9).

The vertical differences in the stress, curvature and elastic modulus of the branch reflect several adaptive significances of tree design.

Table 3-1. Partial and standardized regression coefficients for the multiple regression analysis of elastic modulus (E; $*10^9$ Nm^{-2}) as a function of the depth from the tree top to the branch base (d_{BB}; m), branch length (L_B; m), maximal stress (σ; $*10^6$ Nm^{-2}) and stem inclination (θ; degree). The regression model is $E = b_0 + b_1(d_{BB}) + b_2(L_B) + b_3(\sigma)+b_4(\theta)$, where b_0 is constant, b_n are partial regression coefficients.

Explanatory variables	Partial regression coefficients	Standardized partial regression coefficients	P
(n = 29, R^2 = 0.645, P = 0.0001)			
d_{BB}	-2.595	-1.278	<0.0001
L_B	0.993	0.623	0.0042
σ	2.374×10^{-7}	0.478	0.0269
θ	0.023	0.345	0.0309
Intercept	4.504	4.504	<0.0001

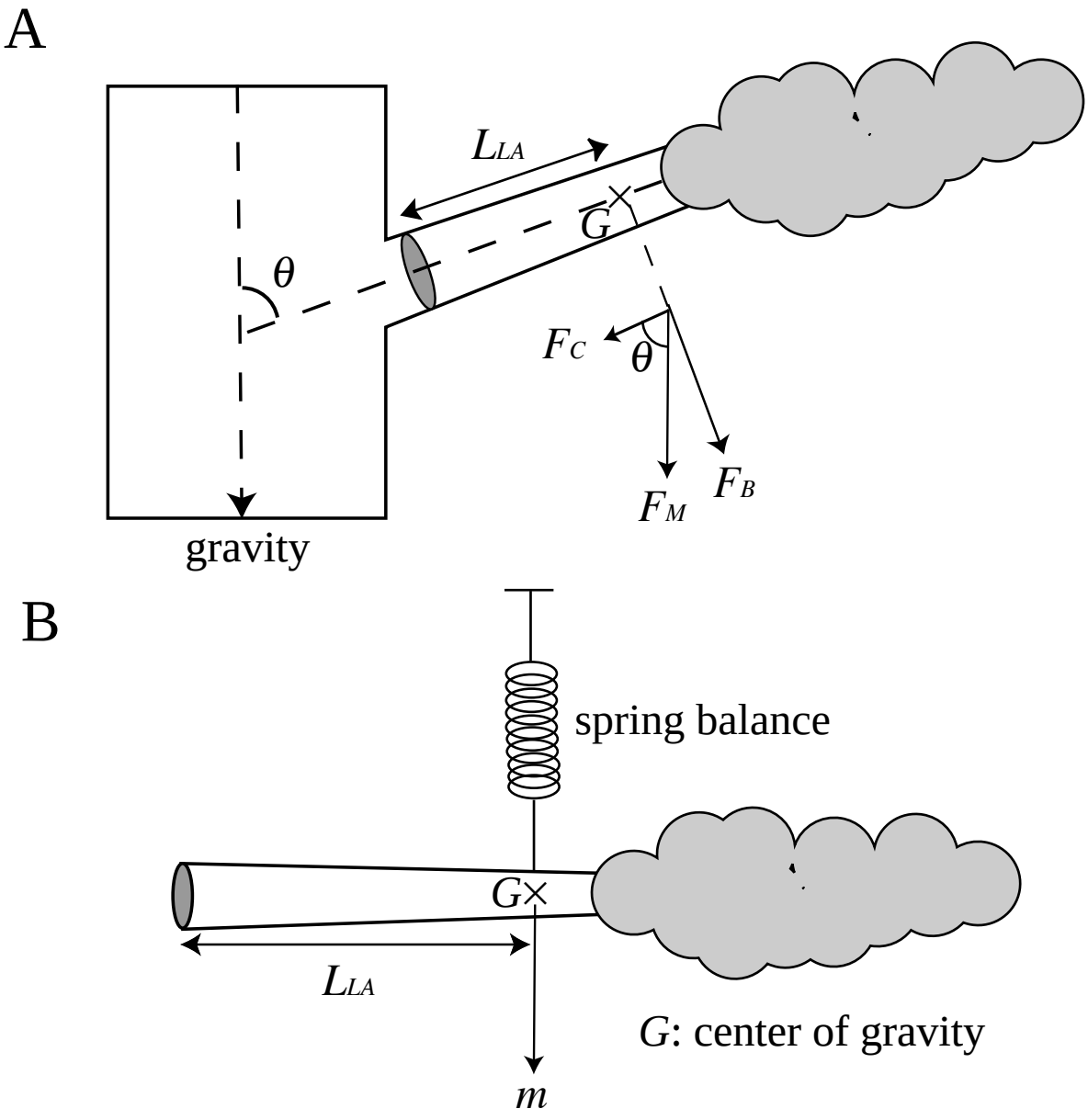

Figure 3-1. Measurement and calculation processes of the bending moment of a branch. A, The branch with an inclination from vertical (θ) is subjected to its own load (F_M). B, Mass of the branch cut at its base (m) was measured with a spring balance at the center of gravity (G) and the length of the lever arm (L_{LA}) that was the distance from the cut base to G was measured. A, The compressive force (F_C) subjecting to the cut cross-section was calculated as $F_M \cos\theta$, and the bending moment (M) subjecting to the cut cross-section was calculated as $L_{LA}\ F_M \sin\theta = L_{LA}\ F_B$.

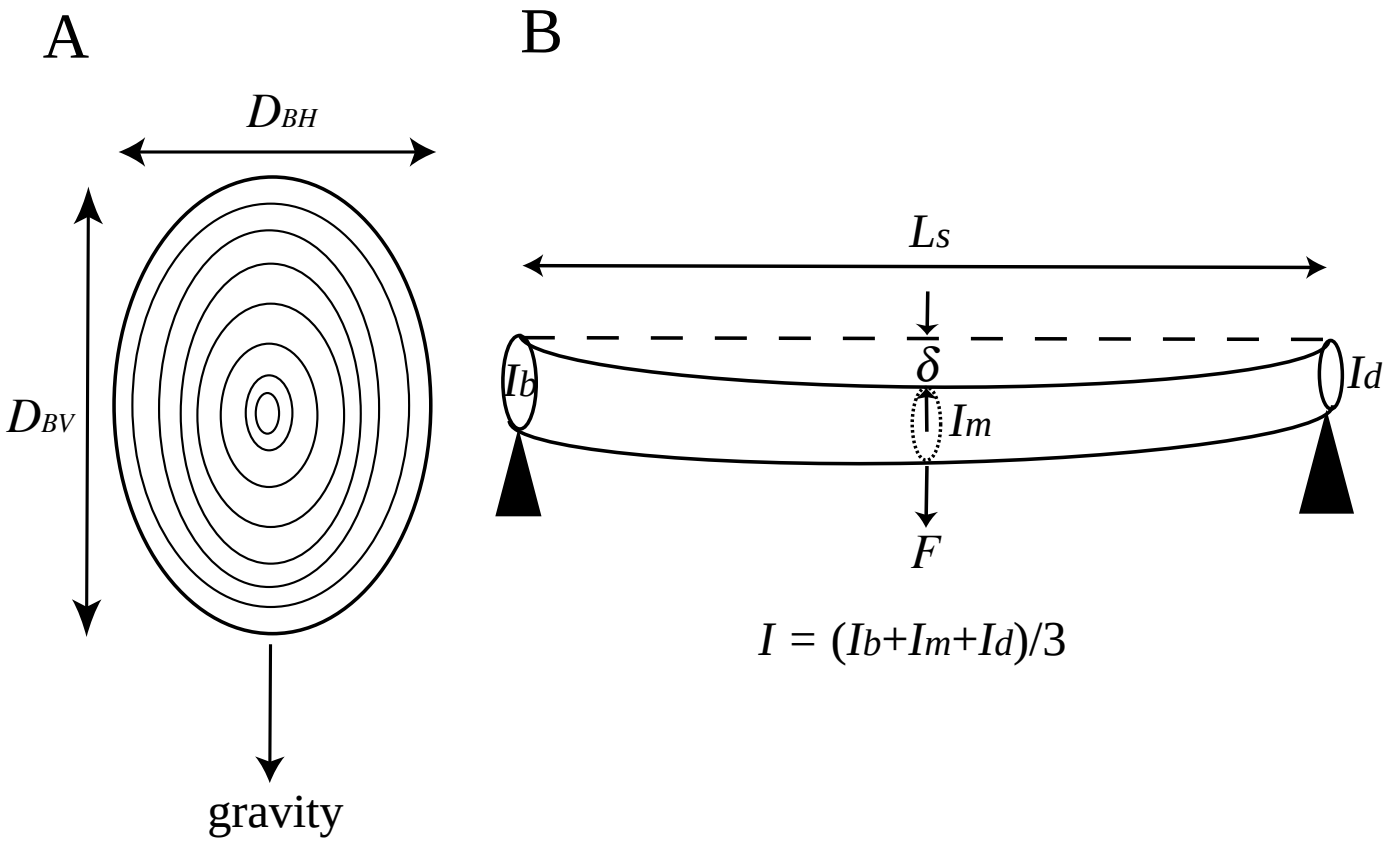

Figure 3-2. Measurement and calculation processes of the elastic modulus and diameters of a branch. A, Diameters of the branch were measured in two directions, vertical diameter (D_{BV}) and horizontal diameter (D_{BH}). B, The fresh specimen of the branch (including bark and phloem) as a beam with an elliptical cross-section was used for determination of the elastic modulus. Each specimen was suspended horizontally across two vertical supports and loaded with force (F) at mid-length with a spring balance. Various loads were applied to each specimen, and corresponding deflections (δ) were measured at midlength. These loads were varied within the elastic range. For calculation of the elastic modulus, the length of the specimen (L_s) and the second moment of area (I) were measured. I was the average of those obtained at distal (I_d), middle (I_m), and basal (I_b) points of the specimen.

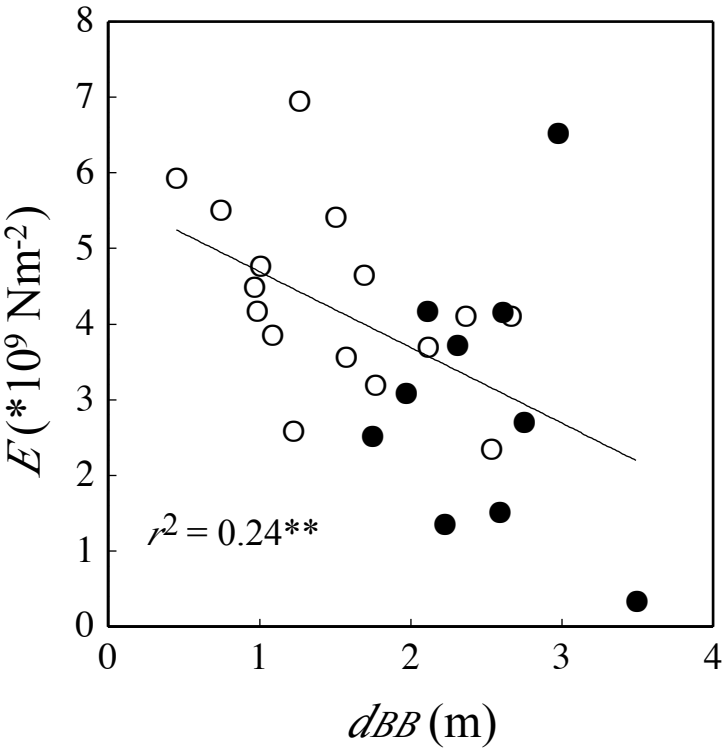

Figure 3-3. Relationships between the elastic modulus (*E*) and the distance from the tree top to branch base (*dBB*). Closed and open symbols indicate stems with leaves and those without leaves, respectively. Linear regression analyses were used ($r2 = 0.24$). **, $p < 0.01$.

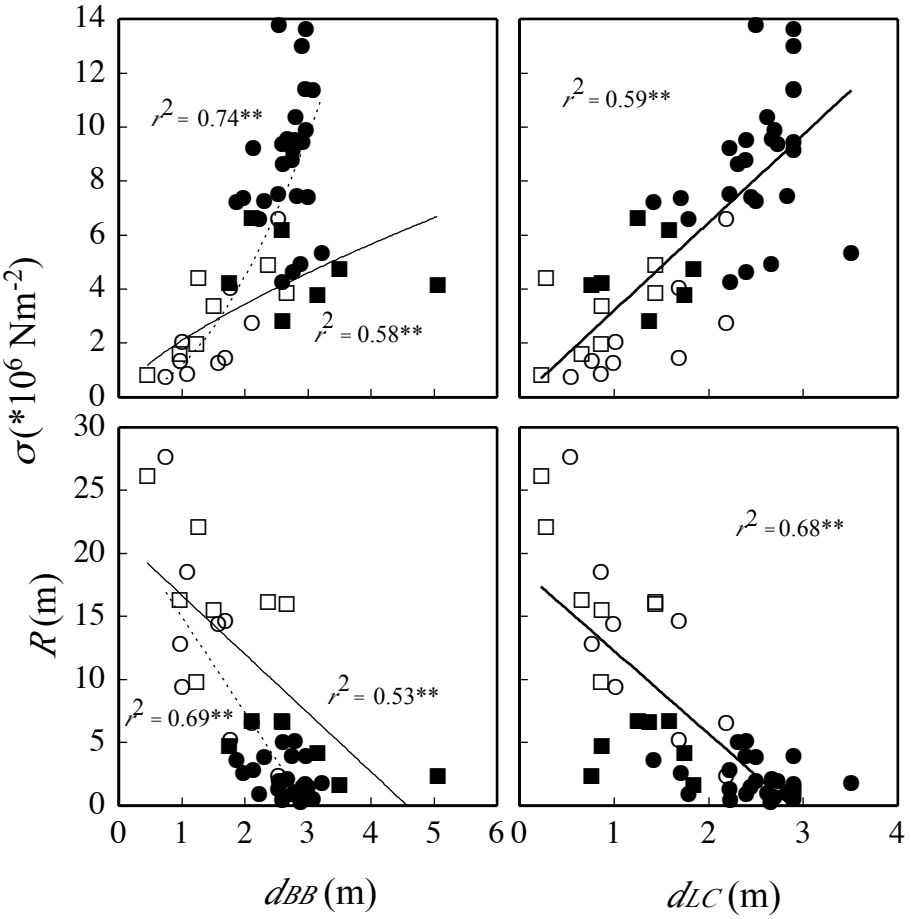

Figure 3-4. Relationships between the mechanical status (σ, stress and R, radius of curvature) and the distance from the tree top to the branch base (dBB, depth of stem base) or to leaf cluster (dLC, depth of leaf cluster). For the relationship between σ and dBB power regression analysis was used. For the other relationships, linear regression analyses were used. Closed and open symbols indicate stems with leaves and those without leaves, respectively. Circles and squares indicate stems of lateral branches and main trunks, respectively. In the left panels, thin solid and dotted lines are regression lines for main trunks and for lateral branches, respectively. Thick solid lines are regression lines for all stems in the right panels. **, $p < 0.01$.

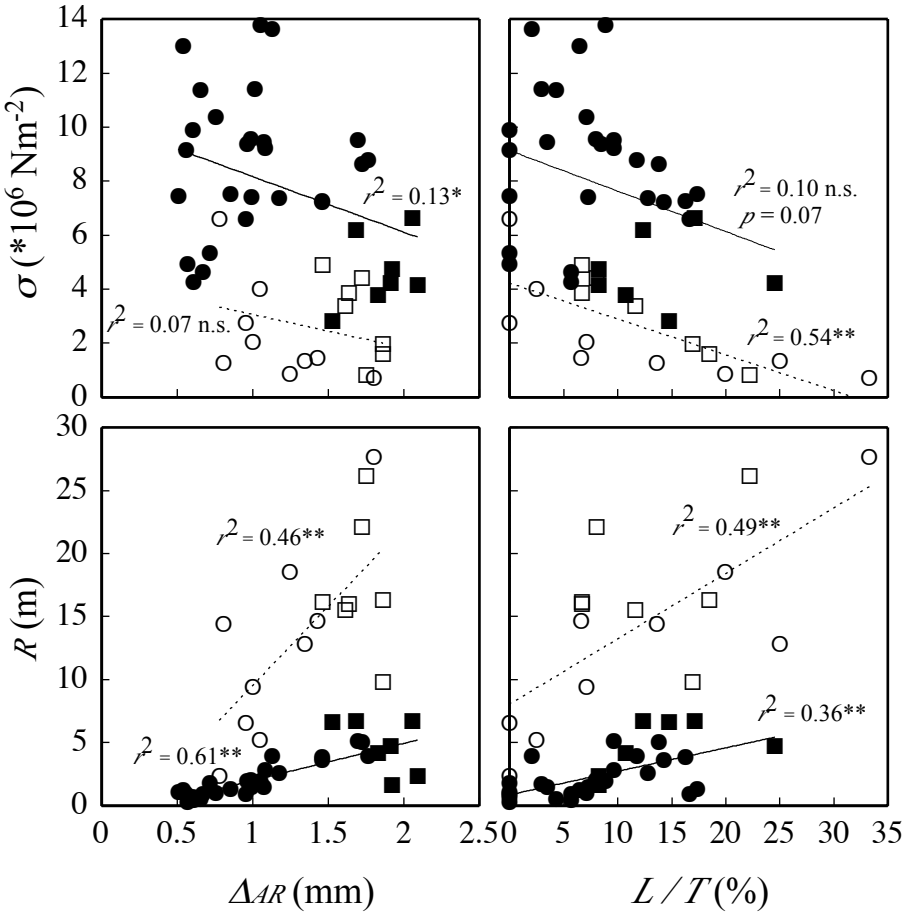

Figure 3-5. Relationships between the mechanical status (σ, stress and R, radius of curvature) and growth activity of the stem (ΔAR, average thickness between annual rings and L/T, number of the long shoots relative to the total number of current-year shoots). Linear regression analyses were used. Symbols are the same as in Figure 3-4. Solid and dotted lines are regression lines for branches with leaves and for those without leaves, respectively. *, $p < 0.05$; **, $p < 0.01$; and n.s., not significant.

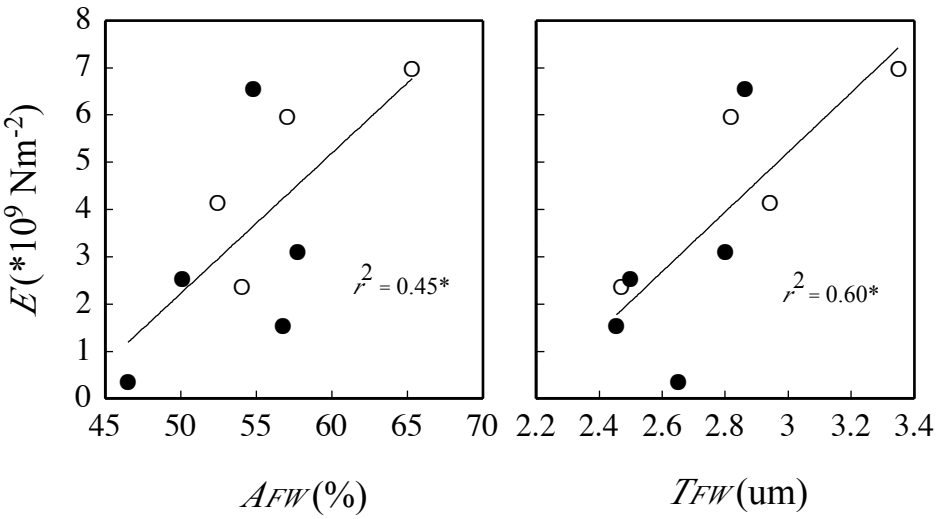

Figure 3-6. Relationships between the elastic modulus (*E*) and properties of fiber cell wall in current-year xylem (*AFW,* area density of fiber cell walls per unit xylem area and *TFW*, average thickness of the fiber cell wall). Symbols are the same as in Figure 3-3. Solid lines are regression lines for all the stems. *, $p < 0.05$.

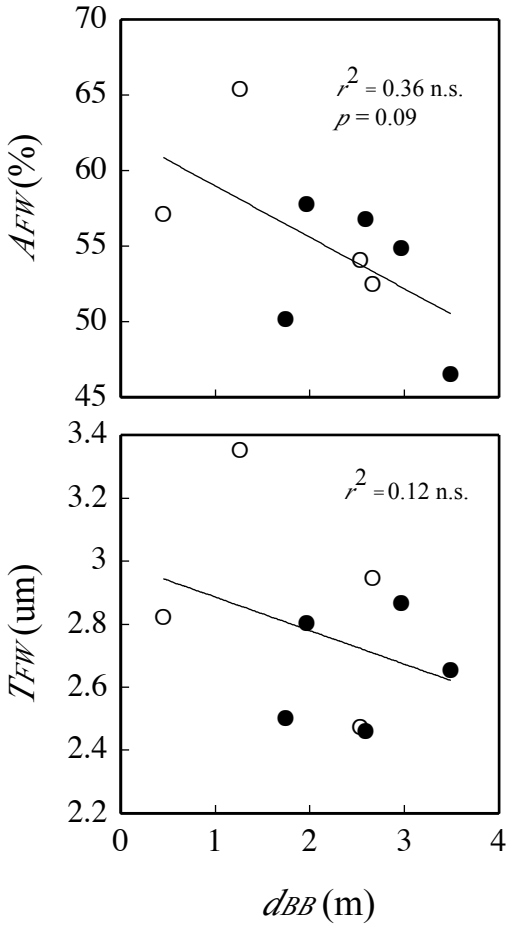

Figure 3-7. Relationships between the properties of fiber cell wall in current-year xylem (*AFW*, area density of fiber cell walls per unit xylem area and *TFW*, average fiber cell wall thickness) and distance from the tree top to the branch base (*dBB*, depth of stem base). Symbols are the same as in Figure 3-3. Solid lines are regression lines for all stems. n.s., not significant.

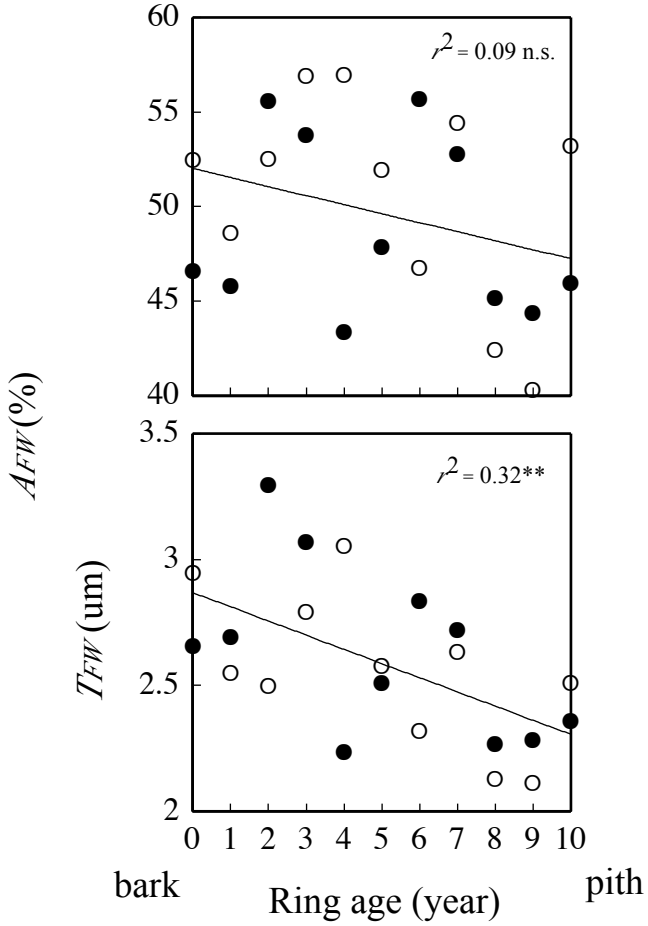

Figure 3-8. Changes in the properties of fiber cell walls (*AFW*, area density of fiber cell walls per unit xylem area and *TFW*, average fiber cell wall thickness) in xylems of main trunks at crown base with the annual ring age. Symbols are the same as in Figure 3-3. Solid lines are regression lines for all the stems. **, $p < 0.01$; n.s., not significant.

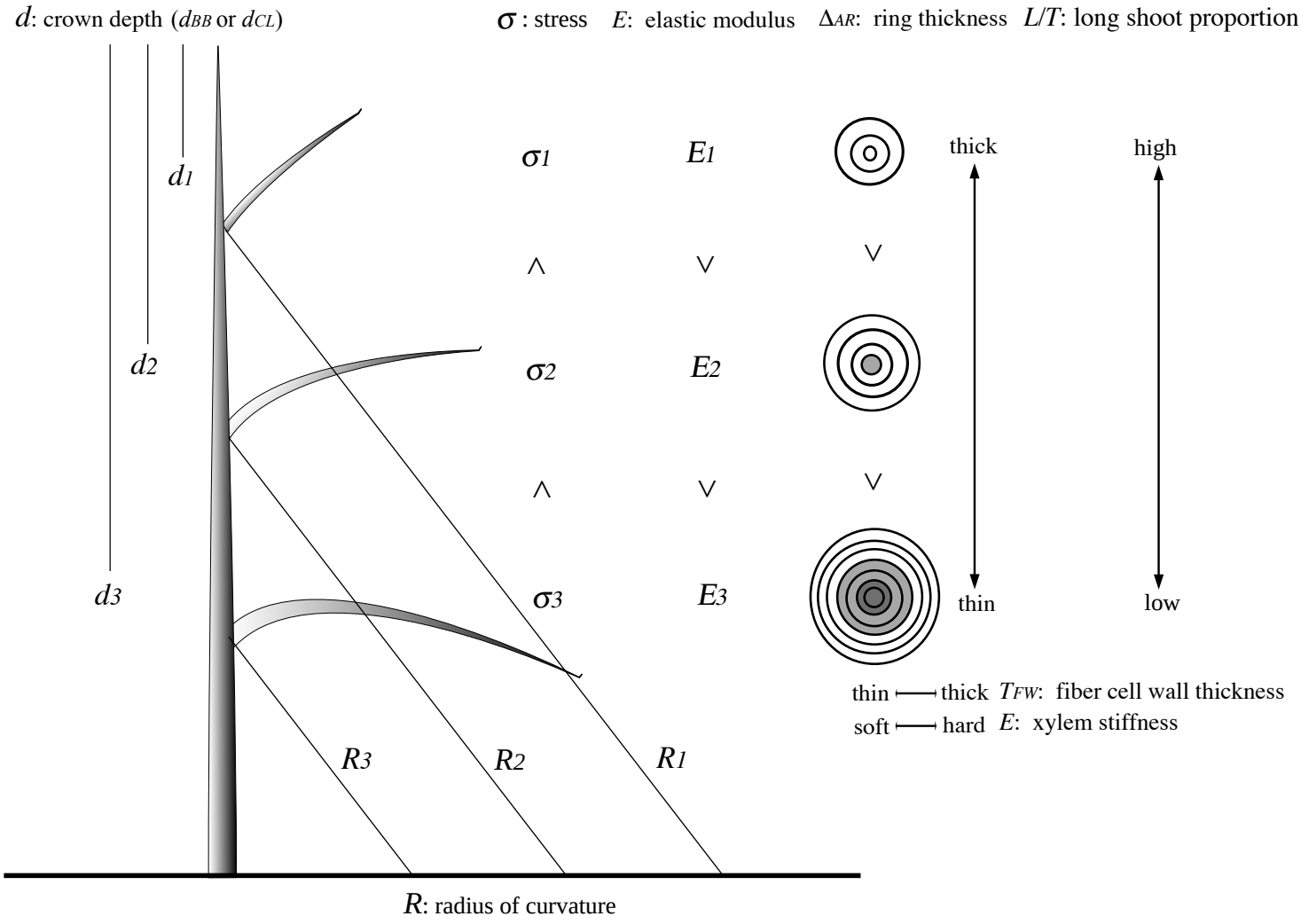

Figure 3-9. A schematic diagram of the mechanical tree design.
Among lateral branches, stress (σ) increases and radius of curvature (*R*) decreases with increment in crown depth (d_{BB} or d_{LC}) and with decrement in growth ring thickness (Δ_{AR}) and long shoot proportion (*L/T*). Elastic modulus (*E*) decreases with increment in crown depth (d_{BB}) because older and inner xylem is softer and has thinner fiber cell walls (T_{FW}).

General Discussion

The tree architecture based on the pipe-model theory can be understood as the balance between supply of and demand for photosynthates at the branch level. In this study, light interception and shoot elongation (or leaf increment) of the branch were used as indices of the supply and demand, respectively. The photosynthates that were produced in each branch depending on its light interception are used in the branch and in downstream organs (Figure G-3). The ratio of the photosynthates consumed in the branch to downward organs depended on branch activity. The dependency of the branch growth on the supply of photosynthates is consistent with "branch autonomy." The concept of branch autonomy is useful for modeling of the tree architecture and/or the forest community structure, because demographic approach can be applied to these problems if the tree individual or forest community is regarded as population of shoot modules. On the other hand, the dependency on the demand for photosynthates highlighted importance of "branch priority". Although importance of the branch priority has been pointed out in relation to shoot elongation, it is also applied to the branch diameter growth. The importance of branch priority in the diameter growth indicates that branches are differentiated and compete actively each other within a tree rather than the paradigm of branch autonomy in which branches are regarded self-supporting units. By dependency on the branch priority, promising branches are sufficiently supported and invested photosynthates for its diameter growth.

This branch priority rule was also applied to the mechanical design of the tree. The productive and promising branches at upper positions are constructed to have smaller mechanical stress and curvature of deflection. Inversely, the unproductive and unpromising branches at lower positions are subject to greater stress and curvature by reduced cost for its diameter growth. Thus, lateral branches are gradually inclined and deflected with tree growth. However, the vertical differentiation of branch inclinations would be effective for photosynthetic production and carbon economy in whole tree level.

In maintenance of the pipe-model architecture, another feature that are different from the above two mechanisms is important. When light intensity, leaf amount or shoot elongation was suppressed, the pipe-model relationship was perturbed. The

diameter growth was declined not only in suppressed branches but also in unsuppressed branches. In the next year of suppression, the pipe-model relationship was recovered by decrement of leaf number and shoot elongation in both branches. The important feature in this recovery should be regard as “branch cooperativeness,” which differs from “branch autonomy” or “branch priority.” The branch cooperativeness is based on the common role of the branches, the allocation of photosynthates into downstream organs such as mother branches, trunks and root systems. Sudden suppression of photosynthetic production in a given branch with relatively large size would cause the increase in the downward translocation from unsuppressed branches. Moreover, the stored matter for the next year growth is pooled and will be allocated to both branches in the next year. By this compensation mechanism, the pipe-model relationship would thus be recovered in the next year.

The branch priority and branch cooperativeness features indicate that the respective branches are interdependent in a tree. The branches within the tree would compete actively each other on one hand but cooperate within the whole tree. The pipe-model architecture is apparently complete and invariance. However, it is dynamically constructed and maintained based on the balance between the branch priority and branch cooperativeness.

Although optimal photosynthetic system of plant canopy have been approached only from viewpoints of leaf arrangement and nitrogen allocation (Monsi and Saeki 1953, 2005, Hirose 2005, Hikosaka 2005), dynamics of the optimum photosynthetic structure which consist of both photosynthetic- and non-photosynthetic- organs was proposed by the present study.

However, further studies are needed to understand the construction mechanisms of tree architecture and thereby its adaptive significance. These features are

(1) responses of the leaf characteristics such as leaf mass per area and nitrogen content, when light intensity, leaf amount or shoot elongation is suppressed.
(2) effects of leaf turnover rate, tree size, branch position on the branch diameter

growth,

and

(3) variations in water transport pathway and vessel connection within a tree and its water conductance.

When information of these features is adequately assessed, we could answer the original question relevant to the pipe-model theory: Why is the stem cross-sectional area proportional to its leaf amount?

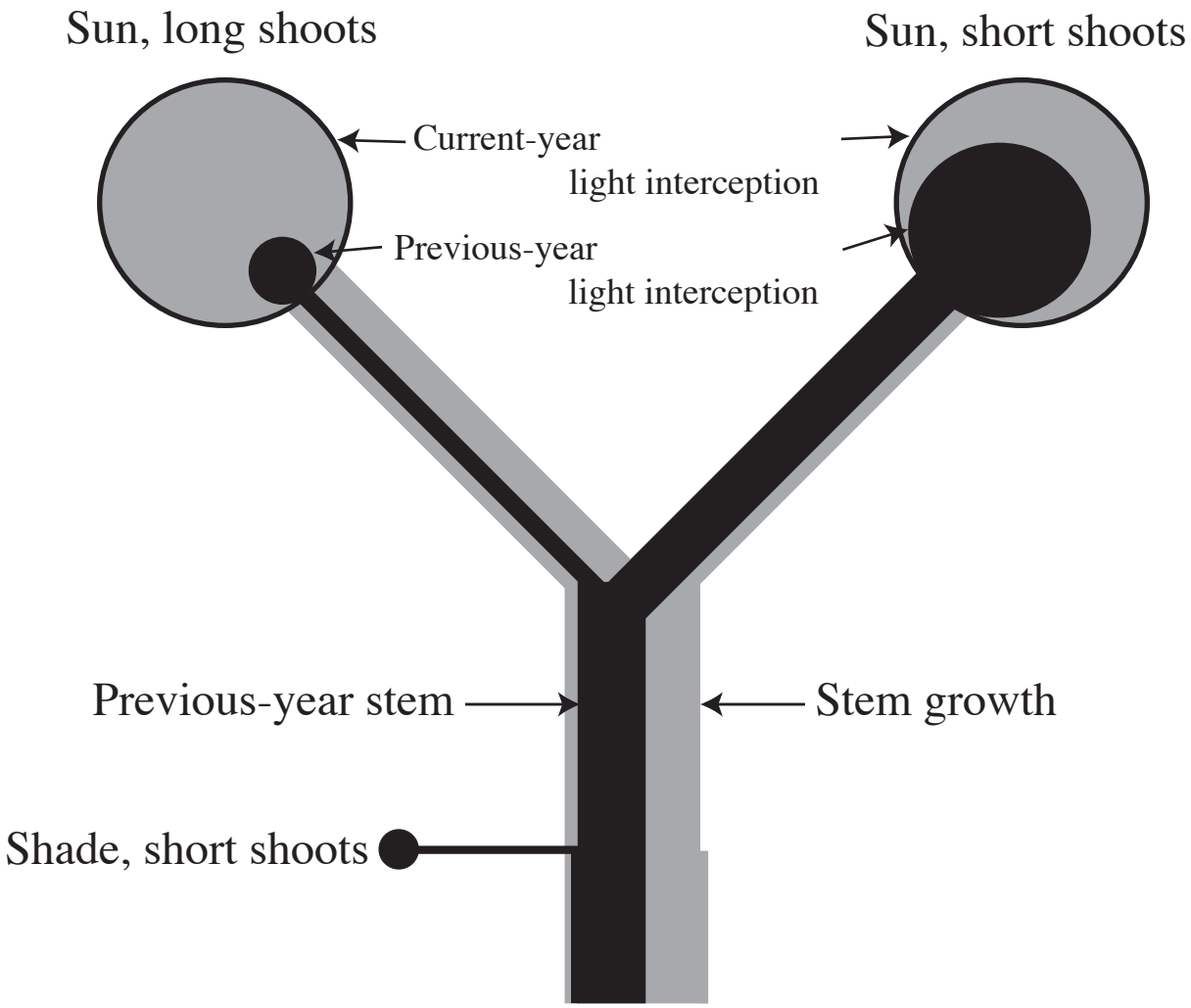

Figure G-3. A model for the branch growth and carbon allocation. Areas of circles indicate cumulated light interceptions by the branches. The shaded and solid circles indicate cumulated light interceptions by the branches in the current year and previous year, respectively. Shaded parts of the stems indicate the wood produced in the current year. Solid parts of the stems denote the wood existed in the previous year (Sone et al. 2005, Terashima et al. 2005).

Acknowledgements

I am grateful to Professor I. Terashima and Dr. K. Noguchi who thoughtful advice and patient encouragement throughout the study. I am also grateful to Professor K. Tsuneki, Associate Professors K. Mizuno, S. Takagi and Dr. T. Asada for constructive comments to this doctoral thesis and Professors I. Washitani and T. Oikawa for significance advice to early version of Chapter 1.

I thank Dr. F. Berninger for reviewing the manuscript of Chapter 1.

I acknowledge Drs. Y. Chiba, Y, Hanba, A. Ishida, S.-I. Ishikawa, H. Muraoka, M. Shibata, A. Takenaka and H. Tanaka for constructive comments for the study. Mr. A. Aoyama and Dr. N. Adachi supplied the instruments for the study. I thank Drs. S. Funayama-Noguchi, S.-I. Miyazawa, A.A. Suzuki, T. Saito, H. Taneda and S. Yano for useful discussion and help my measurement, Drs. T. Ichinose and K. Ando for technical advice about engineering methods. Also, thank to members of Plant Ecophysiology Lab. in Osaka University, of Conservation Ecology Lab. in The University of Tokyo and of Terrestrial Ecology Lab. in University of Tsukuba.

I express my gratitude to Mr. N. Kanagawa, Mr. M. Ryumon and Mrs. F. Sone for assistance for field measurements. The staff of the Ashu Experimental Forest of Kyoto University supported my field study.

I also would like to express my special gratitude to Mrs. Fumie Sone, who is my wife, for supporting my study life.

This research was financially supported by a Sasakawa Scientific Research Grant from the Japan Science Society.

References

Berninger, F. and E. Nikinmaa. 1997. Implications of varying pipe model relationships on Scots pine growth in different climates. Funct. Ecol. 11:146–156.

Berthier, S., A.D. Kokutse, A. Stokes and T. Fourcaud. 2001. Irregular heartwood formation in maritime pine (*Pinus pinaster* Ait): Consequences for biomechanical and hydraulic tree functioning. Ann. Bot. 87:19–25.

Bertram, J.E.A. 1989. Size-dependent differential scaling in branches: the mechanical design of trees revisited. Trees 4:241-253.

Björkman, O. 1981. Responses to different quantum flux densities. *In* Physiological Plant Ecology I: Responses to the physical environment. Eds. O.L. Lange, P. S. Nobel, C.B. Osmond and H. Ziegler. Springer-Verlag, Berlin, pp 57–107.

Campbell, G.S. and J.M. Norman. 1998. Plants and plant communities. *In* An Introduction to Environmental Biophysics, 2nd Edn. Springer-Verlag, New York, pp 223–246.

Cannell, M.G.R., J. Morgan and M.B. Murray. 1988. Diameters and dry weights of tree shoots: effects of Young's modulus, taper, deflection and angle. Tree Physiol. 4:219-231

Carey, E.V., R.M. Callaway and E.H. Delucia. 1998. Increased photosynthesis offsets costs of allocation to sapwood in an arid environment. Ecology 79:2281–2291.

Chiba, Y. 1990. Plant form analysis based on the pipe model theory. I. A statistical model within the crown. Ecol. Res. 5:207–220.

Chiba, Y. 1991. Plant form analysis based on the pipe model theory. II. Quantitative analysis of ramification in morphology. Ecol. Res. 6:21–28.

Chiba, Y. 1998. Architectural analysis of relationship between biomass and basal area based on pipe model theory. Ecol. Model. 108:219–225.

Chiba, Y. 2000. Modelling stem breakage caused by typhoons in plantation *Cryptomeria japonica* forests. For. Ecol. Manage. 135:123-131.

Chiba, Y. and K. Shinozaki. 1994. A simple mathematical model of growth pattern in tree stems. Ann. Bot. 73:91–98.

Chiba, Y., T. Fujimori and Y. Kiyono. 1988. Another interpretation of the profile

diagram and its availability with consideration of the growth process of forest trees. J. Jpn. For. Soc. 70:245–254.

Day, J. and K. Gould. 1997. Vegetative architecture of *Elaeocarpus hookerianus*. Periodic growth patterns in divaricating juveniles. Ann. Bot. 79:607–616.

Dean, T.J. and J.N. Long. 1986. Validity of constant-stress and elastic-instability principles of stem formation in *Pinus contorta* and *Trifolium pratense*. Ann. Bot. 58:833-840.

Domec, J.C. and B.L. Gartner. 2003. Relationship between growth rates and xylem hydraulic characteristics in young, mature and old-growth ponderosa pine trees. Plant Cell Environ. 26:471–483.

Ewers, F.W. and M.H. Zimmermann. 1984a. The hydraulic architecture of balsam fir (*Abies balsamea*). Physiol. Plant. 60:453–458.

Ewers, F.W. and M.H. Zimmermann. 1984b. The hydraulic architecture of eastern hemlock (*Tsuga canadensis*). Can. J. Bot. 62:940–946.

Fushitani, M. 1985. Physics of Wood. Tokyo: Bun-eido. [in Japanese, title translated by the authors.]

Goulet, J., C. Messier and E. Nikinmaa. 2000. Effect of branch position and light availability on shoot growth of understory sugar maple and yellow birch saplings. Can. J. Bot. 78:1077–1085.

Greenhill, A.G. 1881. Determination of the greatest height consistent with stability that a vertical pole or mast can be made, and of the greatest height to which a tree of given proportions can grow. Proc. Cambrid. Philosop. Soc. 4:65-73.

Hanba, Y.T., H. Kogami and I. Terashima. 2002. The effect of growth irradiance on leaf anatomy and photosynthesis in *Acer* species differing in light demand. Plant Cell Environ. 25:1021–1030.

Hikosaka, K. 2005. Leaf canopy as a dynamic system: Ecophysiology and optimality in leaf turnover. Ann. Bot. 95:521-533.

Hirose, T. 2005. Development of the Monsi-Saeki theory on canopy structure and function. Ann. Bot. 95:483-494.

Kershaw, J.A. Jr. and D.A. Maguire. 2000. Influence of vertical foliage structure on the distribution of stem cross-sectional area increment in western hemlock and balsam fir. For. Sci. 46:86–94.

Kikuzawa, K. 1995. Leaf phenology as an optimal strategy for carbon gain in plants. Can. J. Bot. 73:158-163.

Kikuzawa, K., H. Koyama, K. Umeki and M.J. Lechowicz. 1996. Some evidence for an adaptive linkage between leaf phenology and shoot architecture in sapling trees. Funct. Ecol. 10:252-257.

King, D.A. 1986. Tree form, height growth, and susceptibility to wind damage in *Acer saccharum*. Ecol. 67:980-990.

King, D.A. and O.L. Loucks. 1978. The theory of tree bole and branch form. Radiat. Environ. Biophysic. 15:141-165.

King, D.A., E.G. Leigh, R. Condit, R.B. Foster and S.P. Hubbell. 1997. Relationships between branch spacing, growth rate and light in tropical forest saplings. Funct. Ecol. 11:627–635.

Komiyama, A., S. Inoue and T. Ishikawa. 1987. Characteristics of the seasonal diameter growth of twenty-five species of deciduous broad-leaved trees. J. Jpn. For. Soc. 69:379–385. [in Japanese with English summary.]

Komiyama, A., T. Matsuhashi, K. Kurumado and S. Inoue. 1989. Relationships between leaf development and trunk diameter growth in white birch forest. J. Jpn. For. Soc. Chubu Branch 37:51–52. [in Japanese, title translated by the author.]

Koskela, J. 2000. A process-based growth model for the grass stage pine seedlings. Silva Fenn. 34:3–20.

Kozlowski, T.T. and S.G. Pallardy. 1997. Photosynthesis. *In* Physiology of Woody Plants, 2nd Edn. Academic Press, San Diego, pp 87–132.

Li, C., F. Berninger, J. Koskela and E. Sonninen. 2000. Drought responses of *Eucalyptus microtheca* provenances depend on seasonality of rainfall in their place of origin. Aust. J. Plant Physiol. 27:231–238.

Mäkelä, A. 1986. Implications of the pipe model theory on dry matter partitioning and height growth in trees. J. Theor. Biol. 123:103–120.

Mäkelä, A. 1997. A carbon balance model of growth and self-pruning in trees based on structural relationships. For. Sci. 43:7–24.

Mäkelä, A. 1999. Acclimation in dynamic models based on structural relationships. Funct. Ecol. 13:145–156.

Mäkelä, A. 2002. Derivation of stem taper from the pipe theory in a carbon balance

framework. Tree Physiol. 22:891–905.

Mäkelä, A. and P. Vanninen. 1998. Impacts of size and competition on tree form and distribution of aboveground biomass in Scots pine. Can. J. For. Res. 28:216-227.

Mäkelä, A., K. Virtanen and E. Nikinmaa. 1995. The effects of ring width, stem position, and stand density on the relationship between foliage biomass and sapwood area in Scots pine (*Pinus sylvestris*). Can. J. For. Res. 25:970-977.

Matthech, C. and H. Kubler. 1995. Wood – The Internal Optimazation Of Trees. New York: Springer-Verlag.

McDowell, N., H. Barnard, B.J. Bond, T. Hinckley, R.M. Hubbard, H. Ishii, B. Köstner, F. Magnani, J.D. Marshall, F.C. Meinzer, N. Phillips, M.G. Ryan and D. Whitehead. 2002. The relationship between tree height and leaf area: sapwood area ratio. Oecologia 132:12–20.

McMahon, T.A. 1973. Size and shape in biology. Science 179:1201-1204.

McMahon, T.A. and R.E. Kronauer. 1976. Tree structures: Deducing the principle of mechanical design. J. Theor. Biol. 59:443-466.

Mencuccini, M. and J. Grace. 1995. Climate influences the leaf area / sapwood area ratio in Scots pine. Tree Physiol. 15:1–10.

Mencuccini, M., J. Grace and M. Fioravanti. 1997. Biomechanical and hydraulic determinants of tree structure in Scots pine: anatomical sharacteristics. Tree Physiol. 17:105-113.

Messier, C. and P. Puttonen. 1995. Spatial and temporal variation in the light environment of developing Scots pine stands: the basis for a quick and efficient method of characterizing light. Can. J. For. Res. 25:343–354.

Mohr, H. and P. Schopfer. 1995. Plant Physiology, 4th Edn. Springer-Verlag, Berlin.

Monsi, M. and T. Saeki. 1953. Über den Lichtfaktor in den Pflanzengesellschaft- en und seine Bedeutung für die Stoffproduktion. Jpn. J. Bot. 14:22-52.

Monsi, M. and T. Saeki. 2005. On the factor light in plant communities and its importance for matter production. Ann. Bot. 95:549-567.

Morataya, R., G. Galloway, F. Berninger and M. Kanninen. 1999. Foliage biomass–sapwood (area and volume) relationships of *Tectona grandis* L. f. and *Gmelina arborea* Roxb.: silvicultural implications. For. Ecol. Manage. 113:231–239.

Morgan, J. and M.G.R. Cannell. 1988. Support costs of different branch designs: effects of position, number, angle and deflection of laterals. Tree Physiol. 4:303-313.

Morgan, J. and M.G.R. Cannell. 1994. Shape of tree stems – a re-examination of the uniform stress hypothesis. Tree Physiol. 14:49-62.

Murray, C.D. 1927. A relationship between circumference and weight in trees and its bearing on branching angles. J. Physiol. 10:725-739.

Nikinmaa, E. 1992. Analyses of the growth of Scots pine: matching structure with function. Acta For. Fenn. 235: 1–68.

Nikinmaa, E., C. Messier, R. Sievänen, J. Perttunen and M. Lehtonen. 2003. Shoot growth and crown development: effect of crown position in three-dimensional simulations. Tree Physiol. 23:129–136.

Niklas, K.J. 1992. Plant Biomechanics: an engineering approach to plant form and function. Chicago: University of Chicago Press.

Niklas, K.J. 1994. Plant Allometry: the scaling of plant form and process. Chicago: University of Chicago Press.

Niklas, K.J. 1997. Size- and age- dependent variation in the properties of sap- and heartwood in black locust (*Robinia pseudoacacia* L.). Ann. Bot. 79:473-478.

Norberg, R.Å. 1988. Theory of growth geometry of plants and self-thinning of plant populations: Geometric similarity, elastic similarity, and different growth modes of plant parts. Amer. Natural. 131:220-256.

Oohata, S. and K. Shinozaki. 1979. A statistical model of plant form: Further analysis of the pipe model theory. Jpn. J. Ecol. 29:323–335.

Parent, S. and C. Messier. 1996. A simple and efficient method to estimate microsite light availability under a forest canopy. Can. J. For. Res. 26:151–154.

Pearcy, R.W. 1989. Radiation and light measurements. *In* Plant Physiological Ecology—Field methods and instrumentation. Eds. R.W. Pearcy, J. Ehleringer, H.A. Mooney and P.W. Rundel. Kluwer Academic Publishers, Dordrecht, pp 97–116.

Perttunen, J., R. Sievänen, E. Nikinmaa, H. Salminen, H. Saarenmaa and J. Väkevä. 1996. LIGNUM: A tree model based on simple structural units. Ann. Bot. 77:87–98.

Perttunen, J., R. Sievänen and E. Nikinmaa. 1998. LIGNUM: A model combining the structure and the functioning of trees. Ecol. Model. 108:189–198.

Richter, J.P. 1970. The notebooks of Leonardo da Vinci. Dover, New York.

Sakai, S. 1990. Sympodial and monopodial branching in *Acer*: implications for tree architecture and adaptive significance. Can. J. Bot. 68:1549–1553.

Shinozaki, K., K. Yoda, K. Hozumi and T. Kira. 1964a. A quantitative analysis of plant form—the pipe model theory. I. Basic analyses. Jpn. J. Ecol. 14:97–105.

Shinozaki, K., K. Yoda, K. Hozumi and T. Kira. 1964b. A quantitative analysis of plant form—the pipe model theory. II. Further evidence of the theory and its application in forest ecology. Jpn. J. Ecol. 14:133–139.

Sone, K., K. Noguchi and I. Terashima. 2005. Dependency of branch diameter growth in young *Acer* trees on light availability and shoot elongation. Tree Physiol. 25:39-48.

Speck, T.H., H.C. Spatz and D. Vogellehner. 1990. Contributions to the biomechanics of plants. I. Stabilities of plant stems with strengthening elements of different cross sections against weight and wind forces. Bot. Acta 103:111-122.

Sprugel, D.G. 2002. When branch autonomy fails: Milton's law of resource availability and allocation. Tree Physiol. 22:1119–1124.

Sprugel, D.G., T.M. Hinckley and W. Schaap. 1991. The theory and practice of branch autonomy. Annu. Rev. Ecol. System. 22:309–334.

Suzuki, A. 2002. Influence of shoot architectural position on shoot growth and branching patterns in *Cleyera japonica*. Tree Physiol. 22:885-890.

Suzuki, A.A. 2003. Shoot growth patterns in saplings of *Cleyera japonica* in relation to light and architectural position. Tree Physiol. 23:67-71.

Suzuki, M. and T. Hiura. 2000. Allometric differences between current-year shoots and large branches of deciduous broad-leaved tree species. Tree Physiol. 20:203-209.

Takenaka, A. 1994. A simulation model of tree architecture development based on growth response to local light environment. J. Plant Res. 107:321–330.

Takenaka, A. 2000. Shoot growth responses to light microenvironment and correlative inhibition in tree seedlings under a forest canopy. Tree Physiol. 20:987–991.

Taneda, H. and M. Tateno. 2004. The criteria for biomass partitioning of the current shoot: water transport versus mechanical support. Am. J. Bot. 91:1949-1959.

Tateno, M. and K. Bae. 1990. Comparison of lodging safety factor of untreated and succinic acid 2,2-dimethylhydrazide-treated shoots of mulberry tree. Plant Physiol.

92:12-16.

Terashima, I., T. Araya, S.-I. Miyazawa, K. Sone and S. Yano. 2005. Construction and maintenance of the optimal photosynthetic systems of the leaf, herbaceous plant and tree: an eco-developmental treatise. Ann. Bot. 95:507-519.

Terashima, I., K. Kimura, K. Sone, K. Noguchi, A. Ishida, A. Uemura, Y. Matsumoto, Y. 2002. Differential analysis of the effects of the light environment on development of deciduous trees: Basic studies for tree growth modeling. *In:* (*Nakashizuka, T. and Y. Matsumoto eds*) *Diversity and Interaction in a Temperature Forest Community: Ogawa Forest Reserve of Japan*. Ecological Studies, Vol. 158, pp. 187-200, Springer-Verlag, Japan.

Terashima, I. and A. Takenaka. 1986. Organization of photosynthetic system of dorsiventral leaves as adapted to the irradiation from the adaxial side. *In* Biological Control of Photosynthesis. Eds. R. Marcelle, H. Clijsters and M. van Poucke. Martinus Nijhoff Publishers, Dordrecht, pp 219–230.

ter Steege, H. 1994. HEMIPHOT: A programme to analyze vegetation indices, light and light quality from hemispherical photographs. Tropenbos Documents 03. Tropenbos Foundation, Wageningen, the Netherlands.

Valentine, H.T. 1985. Tree-growth models: Derivations employing the pipe-model theory. J. Theor. Biol. 117:579–585.

Valentine, H.T. 2001. Comment: Influence of vertical foliage structure on the distribution of stem cross-sectional area increment in western hemlock and balsam fir. For. Sci. 47:115–116.

Vanninen, P. and A. Mäkelä. 2000. Needle and stem wood production in Scots pine (*Pinus sylvestris*) trees of different age, size and competitive status. Tree Physiol. 20:527–533.

Waring, R.H., P.E. Schroeder and R. Oren. 1982. Application of the pipe model theory to canopy leaf area. J. For. Res. 12:556–560.

West, G.B., J.H. Brown and B.J. Enquist. 1999. A general model for the structure and allometry of plant vascular systems. Nature 400:664–667.

Yamamoto, K. and S. Kobayashi. 1993. Analysis of crown structure based on the pipe model theory. J. Jpn. For. Soc. 75:445–448.

Yoda, K., T. Kira, H. Ogawa and K. Hozumi 1963. Self-thinning in overcrowded pure

stands under cultivated and natural conditions. J. Biol. Osaka City Univ. 14:107-129

Mechanisms of tree architecture construction:
Analyses based on the pipe-model theory and biomechanics

(樹形の構築機構 : パイプモデル理論と生体力学を基盤とした解析)

曽根 恒星 (植物生態生理学研究室)

背景： 樹形に関する経験則に、(1) 枝分かれの前後において枝断面積の合計は等しい (ダ・ヴィンチ則 ; Richter 1970)、(2) 葉の量はその葉のついている枝の断面積に比例する(Shinozaki et al. 1964)、の 2 つがある。篠崎ら(1964)は一般的によく成立するこの 2 つの経験則に基づいて , 樹木個体は一定量の葉を力学的あるいは水供給のために支持するパイプの集合体であると考えた (パイプモデル理論) (図 1)。パイプモデル理論は、樹木成長や水輸送システムの理論研究にさかんに応用されている。

一般に、各枝の光合成産物はその枝よりも下流の幹や根へは転流されるが、他の枝へは転流されない (枝の自律性)。樹形構築のダイナミズムを理解するためには、各枝の光合成産物がその枝と下流の幹や根にどのように分配されているのかを詳しく知る必要がある。一方、工学者や物理学者らは樹木を材質が均一な一本の柱とみなし、力学的ストレスやたわみが一定 (安全率が一定) となるような構造として樹形をとらえてきた。しかし、樹木の成長機構を考慮しつつ各枝の力学的状態の分布様式について詳しく検討した研究はない。

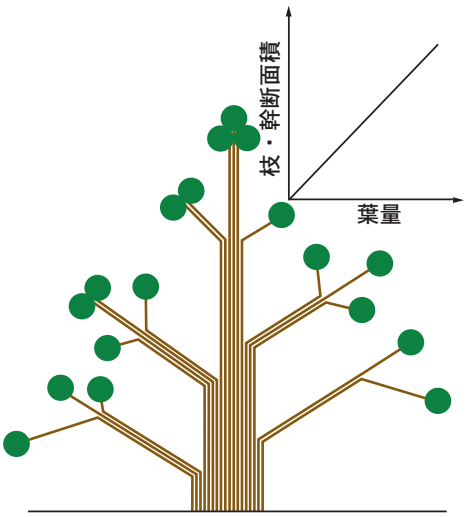

図 1 樹形のパイプモデル

本研究では、これまでの研究ではブラックボックスとして扱われてきたパイプモデル構造の構築・維持機構 (研究 1、2) を解明するとともに枝の力学的状態 (研究 3) も解析し、樹形の構築・維持機構を総合的に理解することを目指した。

研究には、京都大学付属芦生研究林に自生するウリハダカエデ (*Acer rufinerve*、カエデ科落葉広葉樹) の幼木 (樹高 1 ～ 5m) を用いた。この種は、葉齢の区別が不要、当年の肥大成長は主に当年の光合成生産物に依存している、など、本研究に適した性質をもつ。

(研究 1) パイプモデル構造の構築 : 枝の肥大成長の基本ルールについての解析

パイプモデル構造がどのように構築されるのかを明らかにするため、自然環境下での枝の肥大成長についての基本ルールを解析した。各枝の肥大成長、枝の生産量の指標として葉の受光量 (葉面積×光強度)、枝の活力の指標として枝に属する当年枝の平均長と前年に対する葉数の増加量とを測定した。

結果 : 枝の断面積は枝の積算葉面積に比例するが、枝の肥大成長は葉面積にではなく、受光量、当年枝の平均長および前年に対する葉数の増加量に強く依存することが明らかになった。

考察 : 大きな肥大成長を示す枝は、光合成生産が多いと同時に、光合成生産物の需要も大きい。これは、パイプモデル構造は、光合成産物が各枝の需要 (枝の伸長と葉の増加) に応じて配分される結果として構築されていることを示唆している (図 2)。図 2 : 左の枝は需要が高く (伸長が活発で葉の増加も多い) 自身の枝の肥大に光合成産物を優先的に使っている。

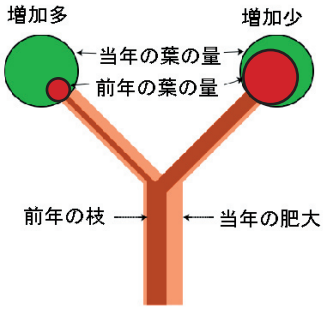

図 2 上部の円は枝の葉量、Y 字の薄い部分は枝の肥大量を示す。

(研究 2) パイプモデル構造の維持 : 光環境、葉・茎の量を操作した時の応答と回復

パイプモデル構造 (枝断面積 / 葉量が一定) の維持メカニズムを明らかにするため、野外のウリハダカエデの光強度、葉量、当年枝長を人為的に操作し、それらがパイプモデル構造にどのような影響をもたらすのかを解析した。2001 年に、調査木を対照個体と処理個体に分け、さらに処理個体を対照枝と処理枝に分けた。この年には操作を行わず、枝ごとの葉数、光強度、枝断面積、年間の枝の伸長量を測定した。2002 年に処理枝に含まれる全ての当年シュートについて被陰、葉を半分に切断、葉を半分摘み取りあるいは当年長枝の摘み取りの操作を行い、2001 年と同じ測定を行った。2003 年には被陰処理のみ継続した。他の操作は行わず、操作からの回復を調べた。

結果 : 長枝の摘み取りを行わずに、葉量や光強度を低下させると枝断面積 / 葉数比 (パイプモデルの比例関係) はやや低下した。興味深いことに、これらの処理木の対照枝においても枝断面積 / 葉数比が低下した。一方、長枝の摘み取りにより葉量と伸長成長の両方を低下させた場合には、枝断面積 / 葉数比は変化しなかった。いずれの処理を行っても、枝断面積 / 葉数比は翌年に回復した。この回復は枝の肥大面積の増大よりも、葉量の抑制によってもたらされた。

考察：これらの結果は、次のように説明出来る（図３；円は当年の葉量または受光量。Y 字部位は枝を示し、薄い部分は当年の肥大量を示す）。葉量や受光量の低下による生産量の低下は枝の肥大を低下させる。しかし、長枝が残っている場合には枝の活発な成長のために光合成産物の需要が大きいので、肥大成長の低下は抑制される（処理枝の生産＜処理枝の需要）。処理枝から下流への光合成産物の転流量の不足分は、対照枝からの転流量の増加（対照枝の生産＞対照枝の需要）によって補償される（中の図）。個体全体の生産抑制により枝への投資は減少し、下流への投資が相対的に増大したため（個体全体の生産＜個体全体の需要）、翌年の伸長と葉の展開が抑えられる。こうして不均衡は解消され（供給と需要との低下による、供給＝需要）、パイプモデル構造は回復、安定化される（右の図）。

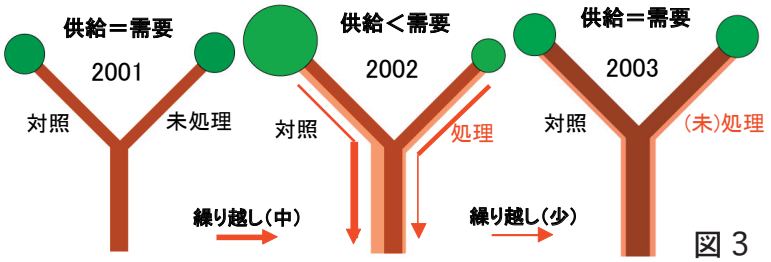

図 3

（研究 3）樹形の力学的バランス：各枝の弾性係数、ストレス、たわみの分布様式

ウリハダカエデ 2 個体（樹高 3m、5m）について、枝に作用する曲げモーメント（= 力×てこの長さ；Nm）、これを受ける枝断面の係数（枝断面の大きさと形で決まる曲げ堅さの係数）、各枝の弾性係数（ヤング率；材質の堅さ）とを測定した。また、木部の解剖学的パラメータ（繊維細胞壁の密度と厚さ）、枝の伸長率および肥大率を測定した。

結果：枝の弾性係数（材質の堅さ）は一定ではなく、下部の枝で低下した。また、弾性係数は、繊維細胞壁の密度と厚さに強く依存していた。下部の枝ではその密度は低下し、枝断面内側の古い木部では細胞壁が薄い傾向があった。枝に作用するストレスやたわみは下部の枝で大きく、また、伸長や肥大の活発な枝ほど小さかった。

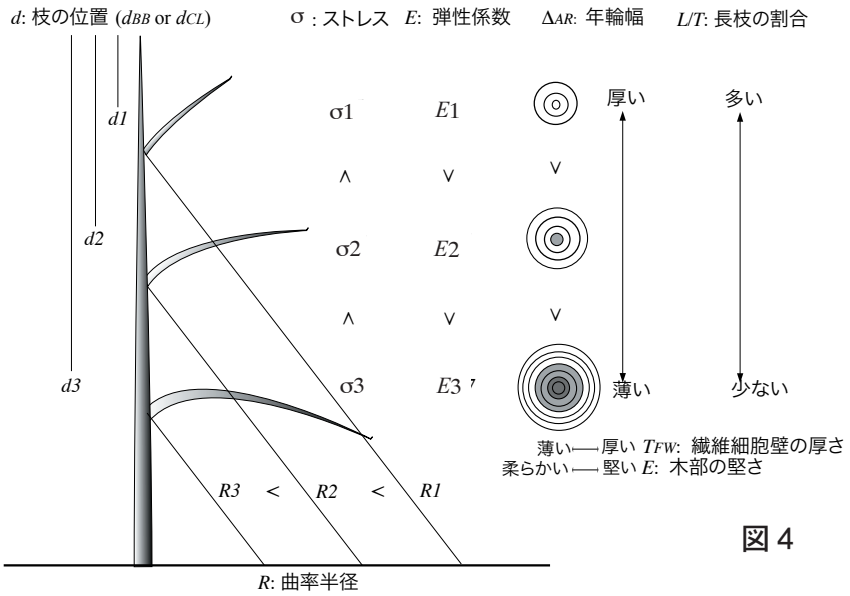

図 4

考察：低い位置の枝の弾性係数の低下とストレス・たわみの増加は、肥大成長の低下にともなう枝の曲げ堅さ（枝の材質と断面の大きさ）の減少が主な原因であろう。下部の枝の肥大のためにコストをかけず水平な状態にたわませることは受光効率と経済性の面でともに効果的である（図４）。

考察：　パイプモデル構造の構築は各枝の生産量と光合成産物の需要の両方に依存していた。前者は「枝の自律性」による樹形構築モデルでも重要視されるが、後者のような「枝の優先性」の性質も重要である。つまり、枝同士は助け合いをしないばかりか競争関係にあり、将来性のある枝は手厚く保護される。この「枝の優先性」のシステムは枝の力学的状態にも反映されていた。個体レベルで考えた場合、上下間の枝の経済性やストレスやたわみの差異による取捨選択は有効な生存戦略である。一方、一部の枝で光環境、葉量、伸長量が抑制されると、パイプモデルの構造は一時的に崩れる。しかし、翌年、抑制された枝だけでなく、抑制されていない枝までも伸長・葉量の低下が起こり、パイプモデル構造が安定化する。これは「枝の優先性」とも、「枝の自律性」とも異なる、いわば「枝の協調性」ともいうべき性質である。翌年の成長に繰り越される生産物が一度プールされ、翌年再び各枝に振り分けられる。この時、枝間の不均衡は補償される。「枝の優先性」と「枝の協調性」のシステムは各枝が個体内で決して独立ではなく、あくまで個体という統合システムの一部に組み込まれていることを示している。個体内の枝は差別化され、激しく競争しながらも個体全体では協調しているのである。このように、静的には普遍的で変化しないかのようにみえるパイプモデル構造であるが、その構築・維持は、実際には非常にダイナミックに行われ、生物学的にも力学的にも枝間の成長の差別化と協調のバランスの上に成り立っているといえる。

発表論文

Sone, K., Noguchi, K., Terashima, I. (2005). Dependency of branch diameter growth in young *Acer* trees on light availability and shoot elongation. *Tree Physiology*. 25:39-48.